INTRODUCTION TO HIGHER ORDER ANALYSIS OF THE ELECTROWEAK INTERACTION*,**

By Z. Hioki

Department of Physics, College of General Education, University of Tokushima, Tokushima 770, Japan

(Received March 25, 1986)

An elementary lecture on electroweak higher order effects is presented. The procedure for renormalizing the electroweak theory on the mass shell is explained. Details of practical one-loop calculations are shown by taking neutrino processes as examples, where treatments of the infrared (IR) and the collinear (CL) divergences are also described. After giving numerical results, an attempt to test clearly for the higher order effects is explained. Applications of this method to heavy particle searches are also shown.

PACS numbers: 11.15.Ex, 12.10.Ck, 13.10.+q, 14.80.Er

CONTENTS

---

* Presented at the IX Silesian School of Theoretical Physics, Szczyrk, Poland, September 22–26, 1985.

** Work supported in part by the Grant-in-Aid for Scientific Research (No. 60740139) from the Ministry of Education, Science and Culture, Japan.

1. Brief view of higher order analysis

1.1. Prologue

The standard $SU(2) \times U(1)$ electroweak theory, i.e., the Glashow–Weinberg–Salam theory [1] has been very successful and widely accepted as the correct theory at least in the zeroth order analyses for low energy phenomena. Moreover, we know at present that it can also describe properly much higher energy processes: e.g., the weak boson production [2]. Therefore, as a next step, much effort should be devoted to testing this theory more precisely, i.e., beyond tree approximation.

Higher order effects (quantum effects) of the electroweak theory have been studied for more than ten years. At an early stage, however, only a small number of people paid attention to them (see, e.g., [3]). That is, this subject was rather an unnoticed one. It is after the phenomenological success of the theory (especially after the discovery of the $W^{\pm}$ and Z bosons [2]) that a lot of particle physicists have become interested in the higher order effects (and their experimental verifications). And, so far, calculations of these effects have been made in $\nu_\mu e \to \nu_\mu e$, $\nu_\mu e \to \mu \nu_e$, $\mu \to e \nu \bar{\nu}$, $\nu q \to \nu q$, $e^+e^- \to l^+l^-$, $e^+e^- \to W^+W^-$, $e^+e^- \to Z\phi$ (ϕ: the Higgs boson), $eq \to eq$, ... (See, e.g., [4, 5] and references cited therein).

These studies will become more and more important since we will obtain, in the near future, a lot of useful information directly from experiments at high energy accelerators: CERN $Sp\bar{p}S$, TRISTAN, SLC, LEP, HERA, Tevatron, ...

In this lecture, I would like to explain the way of renormalizing the electroweak theory (Sect. 2), practical calculations of higher order effects within one-loop approximation (Sect. 3), numerical analysis of them (Sect. 4) (I call these processes simply "renormalization calculations") and also show how to develop a clear experimental test of these effects (Sect. 5). Many parts of this lecture are based on our works:

a) calculations of the electroweak higher order effects for $\nu_\mu e \to \nu_\mu e$, $\bar{\nu}_\mu e \to \bar{\nu}_\mu e$, $\nu_\mu e \to \mu \nu_e$ and $\mu \to e \nu_\mu \bar{\nu}_e$ [6, 7],

b) calculations of the hard photon effects in these processes [8, 9],

c) a proposal to use the weak boson mass relation for testing the higher order effects [10, 11],

d) applications of this mass relation for heavy fermion search [12, 13],

e) review articles [5, 14].

1.2. Summary of renormalization calculations

The process of renormalization calculations consists of several steps: (*i*) Fixing a set of independent parameters, (*ii*) Introducing renormalization constants, (*iii*) Choosing a subtraction scheme to fix the renormalization constants, (*iv*) Practical calculations and (*v*) Determinations of values of parameters. Let us explain each step in the following.

(*i*) Independent parameters

The electroweak theory has five kinds of independent parameters: g, g' (the SU(2) and U(1) coupling constants), μ, λ (the Higgs potential parameters) and g_f (the fermion-Higgs Yukawa coupling constants (matrix)). In the actual calculations, other parameters which are combinations of the above parameters are also used frequently. For example,

g and M_W (the $W^{\pm}$ boson mass) are usually used to describe charged current phenomena, while g, M_Z (the Z boson mass) and $\sin^2\theta_W$ (the Weinberg angle) are adopted for neutral current processes, where, at tree level,

$$M_W = gv/2, \quad M_Z = \sqrt{g^2+g'^2}\,v/2, \quad \sin\theta_W = g'/\sqrt{g^2+g'^2}$$

and

$$v\,(\text{the vacuum expectation value of the scalar field}) = \sqrt{\mu^2/\lambda}. \tag{1.1}$$

We may of course work with any other combination.

In this lecture, I adopt the following set of independent parameters in relation to the on-mass-shell renormalization [5, 7, 15]:

e $(= gg'/\sqrt{g^2+g'^2}$; the electric charge), M_W, M_Z,

$m_f (= g_f v/\sqrt{2}$; the fermion mass matrix), and

$m_\phi (= \sqrt{2\mu^2}$; the Higgs scalar mass).

The Weinberg angle is a very convenient and useful parameter in tree level discussions, but I do not use it since, in addition to the fact that e and masses are more convenient for our scheme, the use of θ_W in higher order analysis sometimes causes a confusion. (I will comment on this point at the end of Sect. 2.)

(*ii*) Renormalization constants

Bare fields, bare masses and bare coupling constants are divided into renormalized ones and divergent parts. In the case of scalar field, for example,

$$\phi_0(x) = Z_\phi^{1/2}\phi(x), \quad m_{\phi 0}^2 = m_\phi^2 + \delta m_\phi^2, \tag{1.2}$$

and in the case of QED,

$$\psi_0(x) = Z_2^{1/2}\psi(x), \quad A_{0\mu}(x) = Z_3^{1/2}A_\mu(x),$$
$$e_0 = Z_1 Z_2^{-1} Z_3^{-1/2} e, \quad m_{\psi 0} = m_\psi + \delta m_\psi. \tag{1.3}$$

Accordingly, the Lagrangian is also divided into the tree part and counterterms,

$$(\phi_0, m_0, \ldots) = \mathscr{L}_{\text{tree}} + \mathscr{L}_{\text{counter}},$$
$$\mathscr{L}_{\text{tree}} = \mathscr{L}(\phi, m, \ldots),$$
$$\mathscr{L}_{\text{counter}} = \mathscr{L}(\phi_0, m_0, \ldots) - \mathscr{L}_{\text{tree}}, \tag{1.4}$$

and the Feynman rules are derived from the tree part.

(*iii*) Subtraction scheme

When making perturbation calculations beyond tree approximation, we frequently meet two kinds of divergences: the ultraviolet (UV) one, and the infrared (IR) one. Further-

more, another divergence also appears when a massless particle emits a massless particle collinearly ("Collinear (CL) divergence" or in other words "mass singularity"). Among these, the UV divergence can be eliminated by suitably adjusting the renormalization constants if the theory is renormalizable. On the other hand, we need other techniques to rescue the theory from the IR and CL divergences, which I will explain in Sect 3.2.

Concerning the determination of the renormalization constants (choice of subtraction scheme), we know at present several ways [16]. As a matter of fact, there are many groups studying electroweak higher order effects, and each has adopted their own scheme which they believe most useful. So, there exist a lot of "the most useful" schemes in the world. If all groups work with a cammon scheme, it will be easy to compare various results with each other, but such a unification, just like a unification of all the languages in the world, will be difficult. Each group will agree only when their own scheme is selected as the standard one.

In the case of the perturbative QCD, the choice of a scheme is not a matter of taste. As is well-known, different schemes produce non-negligible difference in results. Fortunately, however, the scheme dependence is considered to be weak in the case of the electroweak interaction since the expansion parameter, α, is sufficiently small [16]. (Concerning this problem, an interesting paper has recently appeared [17]. See Sect. 5.1 and Sect. 6.) Furthermore there is recently some compromise. That is, there seems to be an emerging consensus on the use of e, M_W, M_Z, m_f and m_ϕ as independent parameters, and renormalizing them by the on-mass-shell conditions [4] although several schemes are still used for determination of wave function renormalization constants.

The scheme which I have been using is the one in which not only the parameters but also all the wave function renormalization constants are fixed by the on-mass-shell conditions [5, 7, 15]. (Such a method is always adopted in the case of QED.) For example, the transverse part of the $W^\pm$ boson self-energy (coefficient of $g_{\alpha\beta}$) is renormalized so that it satisfies

$$\Pi^W(q^2) \text{ and } \Pi^{W'}(q^2) \xrightarrow[q^2 \to M_W^2]{} 0. \tag{1.5}$$

As a result, we obtain the physical mass M_W and a properly normalized (i.e., the pole residue of the propagator = 1) field $W_\mu^\pm(x)$. So, our scheme is the direct and natural extension of the on-mass-shell renormalization in QED, and I of course believe it most useful. A more detailed description is given in the next Section.

(*iv*) Practical calculations

We are now ready to carry out practical calculations. As a method to regularize the UV divergence through computations, the dimensional one is very popular [18]. This method is to keep loop integrals finite by changing the space-time dimension from 4 to D. Then the UV divergence appears in the form $1/\varepsilon$, where $\varepsilon \equiv (4-D)/2$. (This technique is applicable also for the IR divergence.) A lot of concrete examples will be seen in Sect. 3.

(*v*) Determinations of values of parameters

In order to compare the theoretical results with the corresponding experimental data, we have to make numerical computations. Therefore we must determine the values of the parameters first by taking some precisely known experimental data as input.

In the case of the electroweak theory, we need five pieces of data. Let us express them as $f_i^{\exp}$ ($i = 1 \sim 5$). Then, we obtain the following simultaneous equations after calculating f_i theoretically as functions of e, $M_{W,Z}$, m_f and m_ϕ,

$$f_i(e, M_W, M_Z, m_f, m_\phi) = f_i^{\exp}, \tag{1.6}$$

and solving these equations, we can determine the values of those parameters.

If we adopt $e^{\exp}$ ($\equiv \sqrt{4\pi\alpha^{\exp}}$) for $f_1^{\exp}$, the left-hand-side is just e thanks to the on-mass-shell renormalization. Similarly, if we take $M_Z^{\exp}$, $M_W^{\exp}$, ... for $f_2^{\exp}, f_3^{\exp}, \ldots$, then $f_2 = M_Z$, $f_3 = M_W$ ... That is, we can directly substitute the experimental values into the corresponding parameters. Instead of this, if we use, e.g., cross-section of some process σ as one of f_i, the corresponding condition is expressed order by order of perturbation:

$$\sigma^{(\text{tree})}(e, M_W, \ldots) = \sigma^{\exp}$$
$$\Big\downarrow \rightarrow \text{Tree level constraint on } e, M_W, \ldots, \tag{1.7a}$$

$$\sigma^{(1-\text{loop})}(e, M_W, \ldots) = \sigma^{\exp} \tag{1.7b}$$
$$\Big\downarrow \rightarrow \text{One-loop level constraint on } e, M_W, \ldots$$

. . . . . .

(Values of parameters determined by the latter method depend on the choice of input data unless exact quantities are used for the left-hand-side of Eq. (1.6).)

Anyway, after fixing all values of parameters, we can make numerical analysis extensively. A more detailed explanation will be presented in Sect. 4.2.

2. *On-mass-shell renormalization*

In this Section, I will explain the on-mass-shell renormalization procedure. However a great amount of space is necessary to give complete description on it, so the following is only a summary of important points. (For more details, see [5].)

The basic Lagrangian of the electroweak theory consists of four parts:

$$\mathscr{L} = \mathscr{L}_G + \mathscr{L}_F + \mathscr{L}_H + \mathscr{L}_M. \tag{2.1}$$

Here $\mathscr{L}_G$ is the gauge fields part,

$$\mathscr{L}_G = -\tfrac{1}{4} F^a_{\mu\nu} F^{a\mu\nu} - \tfrac{1}{4} F_{\mu\nu} F^{\mu\nu}, \quad (a = 1 \sim 3),$$

$$F^a_{\mu\nu} \equiv \partial_\mu W^a_\nu - \partial_\nu W^a_\mu + g\varepsilon^{abc} W^b_\mu W^c_\nu,$$
(SU(2) gauge fields)

$$F_{\mu\nu} \equiv \partial_\mu w_\nu - \partial_\nu w_\mu, \tag{2.2}$$
(U(1) gauge field)

$\mathscr{L}_{\mathrm{F}}$ is the fermion part,

$$\mathscr{L}_{\mathrm{F}} = \sum_n i\bar{L}_n\gamma^\mu(\partial_\mu - igT^aW_\mu^a - ig'T^0w_\mu)L_n + \sum_n i\bar{R}_n\gamma^\mu(\partial_\mu - ig'T^0w_\mu)R_n, \tag{2.3}$$

where T^a is the SU(2) generators, and T^0 is determined by $T^3+T^0 = Q_{\mathrm{f}}$ (electric charge of a fermion f in the proton charge e unit), and

$$L \equiv \begin{pmatrix} \psi_I \\ \psi_i \end{pmatrix}_{\mathrm{L}}, \qquad R \equiv \psi_{\mathrm{R}},$$

(I have used I and i to express the weak isospin $+\frac{1}{2}$ and $-\frac{1}{2}$ component respectively.) $\mathscr{L}_{\mathrm{H}}$ is the Higgs scalar part,

$$\mathscr{L}_{\mathrm{H}} = |(\partial_\mu - igT^aW_\mu^a - ig'T^0w_\mu)\Phi|^2 + \mu^2\Phi^\dagger\Phi - \lambda(\Phi^\dagger\Phi)^2,$$
$$\Phi = \frac{1}{\sqrt{2}}\begin{pmatrix} i\chi_1+\chi_2 \\ v+\phi-i\chi_3 \end{pmatrix}, \tag{2.4}$$

where χ_i ($i = 1 \sim 3$) and ϕ are scalar fields which become the Nambu–Goldstone bosons and the physical Higgs field respectively after the spontaneous symmetry breakdown, and $\mathscr{L}_{\mathrm{M}}$ is the mass generating term,

$$\mathscr{L}_M = -g_{\mathrm{f}_{mn}}\bar{L}_m\Phi R_n - g'_{\mathrm{f}_{mn}}\bar{L}_m(i\tau_2\Phi^*)R_n + (\mathrm{h.c.}), \tag{2.5}$$

where the first (the second) term gives a mass to $T^3 = -1/2$ $(+1/2)$ component fermions. In addition to these terms, we have to take account of the gauge fixing term $\mathscr{L}_{\mathrm{GF}}$ and the Fadeev–Popov ghost term $\mathscr{L}_{\mathrm{FP}}$ to make the electroweak theory "a consistent quantum field theory"

$$\mathscr{L}[\mathrm{EW}] = \mathscr{L}_{\mathrm{G}} + \mathscr{L}_{\mathrm{F}} + \mathscr{L}_{\mathrm{H}} + \mathscr{L}_{\mathrm{M}} + \mathscr{L}_{\mathrm{GF}} + \mathscr{L}_{\mathrm{FP}}. \tag{2.6}$$

After the spontaneous symmetry breakdown, mass terms are generated, and by diagonalizing them $\mathscr{L}$ is re-expressed in terms of the mass eigenstates $W_\mu^\pm$, Z_μ, A_μ, ψ and ϕ (and several unphysical particles). At the same time, we of course transform g, g', ..., g_{f} to e, M_{W}, M_{Z}, m_{f} and m_ϕ. According to the diagonalization of the fermion mass matrix, the Kobayashi–Maskawa mixing matrix U_{Ii} is also introduced.

As a next step, let us introduce renormalization constants. We should pay special attention to the neutral gauge boson (the Z boson and the photon A) and the fermion sectors since so-called "particle mixing" occurs. For example, concerning the Z boson-photon sector, the Z–A transition self-energy diagram (Fig. 2.1) gives non-zero contribu-

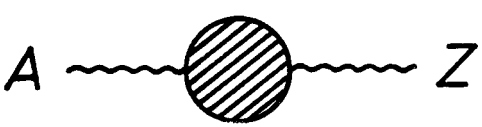

Fig. 2.1. The A(photon) — Z boson transition self-energy

tion. It is natural to renormalize so that its contribution vanishes for $q^2 = 0$ and $q^2 = M_Z^2$. In order to realize it, we have to use matrix type renormalization constants (also for the fermion sectors) as follows:

$$\begin{pmatrix} Z_{0\mu} \\ A_{0\mu} \end{pmatrix} = \begin{pmatrix} Z_{ZZ}^{1/2} & Z_{ZA}^{1/2} \\ Z_{AZ}^{1/2} & Z_{AA}^{1/2} \end{pmatrix} \begin{pmatrix} Z_\mu \\ A_\mu \end{pmatrix} \quad (Z_{ZA} \neq Z_{AZ}), \tag{2.7}$$

$$\psi_{0L,R}^n = (Z_{L,R}^{1/2})^{nm} \psi_{L,R}^m \quad (Q_n = Q_m). \tag{2.8}$$

For other quantities,

$$M_{Z0}^2 = M_Z^2 + \delta M_Z^2$$

$$W_{0\mu}^{\pm} = Z_W^{1/2} W_\mu^{\pm}, \quad M_{W0}^2 = M_W^2 + \delta M_W^2,$$

and

$$e_0 = Ye. \tag{2.9}$$

The renormalization constants for the Higgs scalar, the Nambu–Goldstone bosons and the FP ghosts are also introduced in a similar way. (Concerning the FP ghosts, a simpler treatment is possible due to the fact that they appear only in loops.) Consequently the Lagrangian is divided into two parts:

$$\mathscr{L} = \mathscr{L}_{\text{tree}} + \mathscr{L}_{\text{counter}}. \tag{2.10}$$

In the following, I show the renormalization conditions and counterterms for the gauge boson sector explicitly. Let us represent the transverse parts of the renormalized $W^{\pm}$, Z, A and Z–A proper self-energies as

$$\Pi^W(q^2), \quad \Pi^Z(q^2), \quad \Pi^A(q^2) \quad \text{and} \quad \Pi^{ZA}(q^2)$$

respectively. They consist of the unrenormalized self-energies $\Pi_{(U)}^W$, $\Pi_{(U)}^Z$, $\Pi_{(U)}^A$ and $\Pi_{(U)}^{ZA}$, and the corresponding counterterms. For example, at one-loop level,

$$\Pi^W(q^2) = \Pi_{(U)}^W(q^2) + \delta M_W^2 + Z_W(M_W^2 - q^2), \tag{2.11a}$$

$$\Pi^Z(q^2) = \Pi_{(U)}^Z(q^2) + \delta M_Z^2 + 2Z_{ZZ}^{1/2}(M_Z^2 - q^2), \tag{2.11b}$$

$$\Pi^A(q^2) = \Pi_{(U)}^A(q^2) - 2Z_{AA}^{1/2} q^2, \tag{2.11c}$$

$$\Pi^{ZA}(q^2) = \Pi_{(U)}^{ZA}(q^2) + Z_{ZA}^{1/2}(M_Z^2 - q^2) - Z_{AZ}^{1/2} q^2, \tag{2.11d}$$

where all renormalization constants mean the order α terms in the perturbation expansion of those in Eqs. (2.7) and (2.9).

We impose the on-mass-shell conditions on them:

$$\text{Re}\,\Pi^W(M_W^2) = \text{Re}\,\Pi^{W'}(M_W^2) = 0, \tag{2.12}$$

$$\text{Re}\,\Pi^Z(M_Z^2) = \text{Re}\,\Pi^{Z'}(M_Z^2) = \text{Re}\,\Pi^{ZA}(M_Z^2) = 0,$$

$$\Pi^A(0) = \Pi^{A'}(0) = \Pi^{ZA}(0) = 0. \tag{2.13}$$

Here in the six conditions of Eq. (2.13), only five are linearly independent due to the remaining U(1) gauge symmetry. Actually, $\Pi^{A}_{(U)}(0) = 0$ and there is no corresponding counterterm at one-loop level. We obtain the following results[1]

$$\delta M_W^2 = -\Pi^{W}_{(U)}(M_W^2), \quad Z_W = \Pi^{W'}_{(U)}(M_W^2),$$

$$\delta M_Z^2 = -\Pi^{Z}_{(U)}(M_Z^2), \quad Z_{ZZ}^{1/2} = \tfrac{1}{2}\Pi^{Z'}_{(U)}(M_Z^2),$$

$$Z_{AA}^{1/2} = \tfrac{1}{2}\Pi^{A'}_{(U)}(0), \quad Z_{AZ}^{1/2} = \frac{1}{M_Z^2}\Pi^{ZA}_{(U)}(M_Z^2), \quad Z_{ZA}^{1/2} = \frac{-1}{M_Z^2}\Pi^{ZA}_{(U)}(0). \tag{2.14}$$

We can renormalize similarly the fermion sector and the Higgs sector.

On the other hand, the unphysical particles do not appear in external lines, so the finite parts of their renormalization constants are irrelevant. Hence we may take any renormalization condition. All we have to do is to eliminate the corresponding divergences. Practically the minimal subtraction is most convenient.

Finally we obtain the physical parameters e, M_W, M_Z, m_f and m_ϕ, and the properly normalized fields $W_\mu^{\pm}(x)$, $Z_\mu(x)$, $A_\mu(x)$, $\psi_{L,R}(x)$ and $\phi(x)$. After practical calculations, all physical quantities are expressed in terms of the above physical parameters.

I did not adopt the Weinberg angle as one of the independent parameters so let us comment on this point before proceeding to the next section. As is well-known, $\sin^2\theta_W$ is a very useful parameter in tree level analysis. As a matter of fact, the structure of the neutral currents is expressed very clearly, and we can write various relations among parameters very simply with a help of θ_W.

Beyond tree approximation, however, it is no longer true. When we say "mass" or "electric charge", you will naturally think of the physical ones, i.e., those defined on the mass shell. And, there is the unique (process-independent) correspondence between theory and experiment: In the case of mass, for example, the real part of the pole of the propagator and the peak point of the corresponding invariant mass distribution (e.g., $M_Z \rightleftarrows$ the peak of $M(e^+e^-)$ for $Z \to e^+e^-$). However, the Weinberg angle does not have such a property, and consequently there has been so far no natural "standard definition" of it. Different definitions have often been used in different papers, and we sometimes meet a comment like;

"Their results differ somewhat from ours in part because a different definition of $\sin^2\theta_W$ was employed".

We can see a typical example of such a confusion in the relations among M_W, M_Z, θ_W and the ϱ-parameter which are frequently discussed after the discovery of $W^{\pm}$ and Z: In one scheme (Appelquist et al. and Salomonson-Ueda in [3]), the well-known relation $M_W = M_Z \cos\theta_W$ receives a radiative correction

$$M_W = M_Z \cos\theta_W + O(\alpha),$$

[1] There are some incomplete parts in the descriptions of our review article [5], and we need modifications when making two-loop analysis [19]. Fortunately, however, no parts of our previous works are affected.

while in another scheme [20],

$$M_W = M_Z \cos\theta_W,$$

where $M_{W,Z}$ are the physical masses in both cases (in the latter scheme, this equation is just the definition of θ_W and it may be the standard one in the future). Furthermore ϱ is sometimes expressed as $\varrho \equiv M_W^2/(M_Z^2 \cos^2\theta_W)$ and a deviation of ϱ from 1 by radiative correction is discussed.

Of course, this discussion never means any logical inconsistency, and we can obtain correct results in a scheme with θ_W. However, it is desirable to avoid such a confusion. This is the other reason why I did not use θ_W. Then, readers may have a question: "A lot of experimental data have been reported in terms of θ_W. What does this θ_W mean?" The answer is as follows: Experimentalists express their results on measurements of cross-sections, decay-widths, asymmetries etc. in terms of θ_W through the tree level formulas. So, its meaning is apparent. We should distinguish clearly θ_W as a parameter in theoretical calculations and θ_W as experimental data (which I hereafter express as "θ_W^{exp}"). Discussions in Sect. 4.2 will be useful for understanding this situation (there I will give the definition of ϱ too).

3. *One-loop effects: practical calculations*

I show, in this Section, practical calculations of electroweak higher order effects within one-loop approximation taking purely leptonic neutral current processes, $\nu_\mu(\bar{\nu}_\mu)e \to \nu_\mu(\bar{\nu}_\mu)e$ and charged current processes, $\nu_\mu e \to \mu\nu_e$ ($\mu \to e\nu_\mu\bar{\nu}_e$) as examples. From the theoretical point of view, they are the most suitable examples since their structures are very simple and strong interaction effects are considered not so important (although more accurate experimental information is obtained from deep inelastic ν_μ-nucleon scatterings).

As was mentioned in Sect. 1 we will meet two kinds of divergences: One is the UV divergence, which arises from high momentum region in loop integrals and is eliminated by renormalization. The others are the IR and CL divergences, which have their origin in low energy region, i.e., occur due to the existence of massless particles, and we have to take account of additional diagrams (real photon emission in the present case) in order to rescue the theory [21].

I should also mention regularization of divergences since, practically, we cannot make any well-defined computation in intermediate stages without regularizing divergences. In order to regulate the UV divergence, I adopt the dimensional method briefly explained in Sect. 1.2. The IR divergence can be also treated by this technique, but I will use a traditional one, in which a small fictitious photon mass λ is introduced, to show a procedure different from dimensional one. Consequently, the IR divergence appears in the form of $\ln\lambda$. On the other hand, the CL divergence is an approximate one in our case, i.e., becomes "real divergence" only in the limit m_e or $m_\mu \to 0$. It appears, e.g., in the form $\sim (\ln m_e)^2$ in $\nu_\mu e \to \nu_\mu e$ process. So, regularization is unnecessary.

3.1. UV divergence and renormalization

In the neutrino-lepton processes, the squared momentum transfer q^2 is very much smaller than $M^2_{W,Z}$. In fact, the mean value is estimated to be $|\langle q^2 \rangle| \sim 4$–$5\,(\mathrm{GeV})^2$ even at $E_\nu^{\mathrm{Lab}} = 10^4$ GeV. Therefore I neglect quantities of $O(q^2/M^2_{W,Z})$, and also those of $O(m_{e,\mu}/M_{W,Z})$ in comparison with $O(1)$ quantities. Thanks to this reasonable approximation, we may leave out of consideration every diagram with the Higgs-lepton vertex since this coupling is proportional to $m_{e,\mu}/M_{W,Z}$. Then we obtain the relevant Feynman diagrams for $\nu_\mu(\bar{\nu}_\mu)e \to \nu_\mu(\bar{\nu}_\mu)e$ process (Fig. 3.1) and for $\nu_\mu e \to \mu\nu_e$ ($\mu \to e\nu_\mu\bar{\nu}_e$) process (Fig. 3.2). There blobs stand for all the possible one-loop diagrams, which are explicitly shown in the following. I discuss the neutral current processes first.

Neutral current processes

Let us first arrange the necessary renormalization constants (within one-loop approximation):

For the Z boson self-energy (Fig. 3.1(2)),

$$\delta M_Z^2, \quad Z_{ZZ}^{1/2};$$

for the Z–A transition self-energy (Fig. 3.1(3)),

$$Z_{ZA}^{1/2}, \quad Z_{AZ}^{1/2};$$

(These four constants are determined here.)

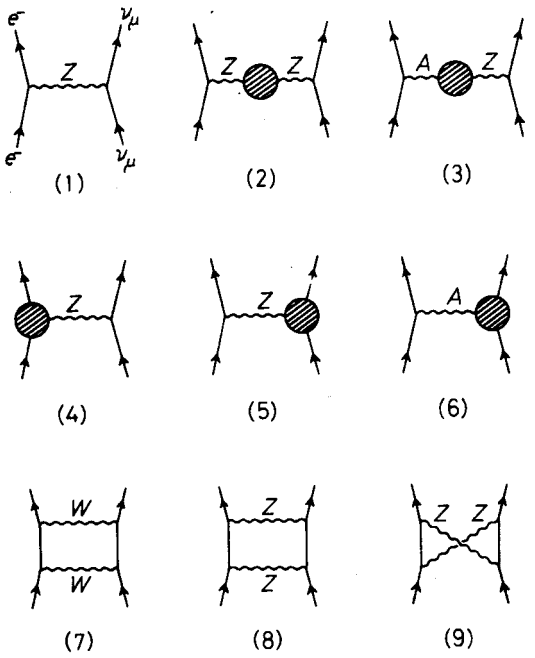

Fig. 3.1. Relevant diagrams of one-loop corrections for the process $\nu_\mu(\bar{\nu}_\mu)e \to \nu_\mu(\bar{\nu}_\mu)e$

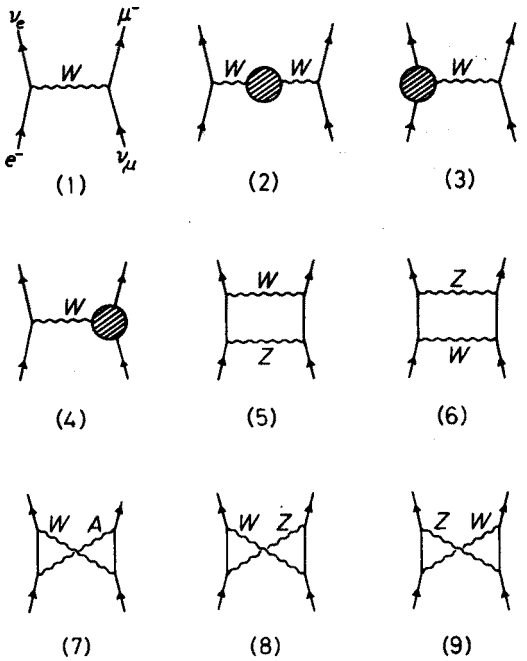

Fig. 3.2. Relevant diagrams of one-loop corrections for the process $\nu_\mu e \to \mu\nu_e(\mu \to e\nu_\mu\bar{\nu}_e)$

for the eeZ vertex (Fig. 3.1(4))[2],

$$Y, \delta M_W^2, Z_L^e, Z_R^e \text{ (and already fixed } Z_{ZZ}^{1/2}, Z_{AZ}^{1/2}, \delta M_Z^2);$$

for the $\nu\nu$Z vertex (Fig. 3.1(5)),

$$Y, \delta M_W^2, Z_L^\nu \text{ (and } Z_{ZZ}^{1/2}, \delta M_Z^2);$$

for the $\nu\nu$A vertex (Fig. 3.1(6)),

$$(Z_{ZA}^{1/2}).$$

In order to determine Y, δM_W^2, $Z_{L,R}^e$, Z_L^ν, we have to take account of additional diagrams:
the $W^\pm$ boson self-energy for δM_W^2 (see CC.1),
the lepton (e and ν) self-energy for $Z_{L,R}^e$ and Z_L^ν,
the eeA vertex for Y.

In the following, I show one-loop diagrams for each blob of Fig. 3.1, and the corresponding formulas in the 't Hooft-Feynman gauge. (Explicit formulas for the renormalization constants will be collected in Appendix A.2.)

---

[2] In the present case, we need only diagonal elements of $Z_{L,R}^{mn}$ for electron and muon, and those of Z_L^{mn} for neutrinos. I represent them as $Z_{L,R}^l$ (l = e or μ) and Z_L^ν in the following.

NC. 1. Z boson self-energy

Twelve kinds of diagrams contribute (Fig. 3.3),

$$\Pi^{Z}(q^2) = \sum_{n=1}^{12} \Pi^{Z}_{(U)n}(q^2) + \Pi^{Z}_{C}(q^2). \tag{3.1}$$

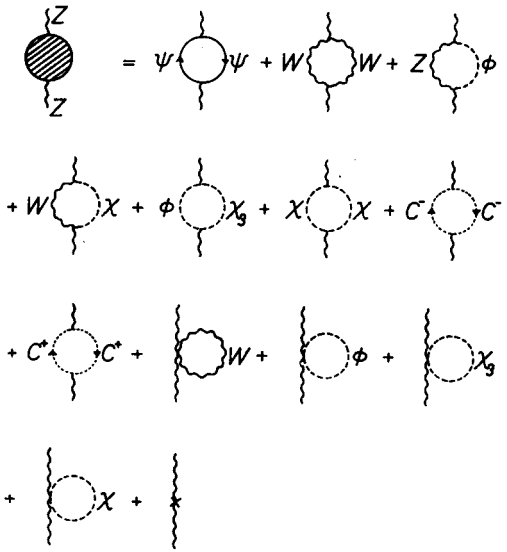

Fig. 3.3. The Z boson self-energy at one-loop level. $C^{\pm}$ represent the FP ghosts, and the last diagram expresses the counterterm

Here, the second term is the counterterm, and

$$\Pi^{Z}_{(U)}(q^2) = \sum_{n=1}^{12} \Pi^{Z}_{(U)n}(q^2) = \frac{\alpha}{8\pi M_W^2(M_Z^2 - M_W^2)} \Bigg[\sum_{f} M_Z^4 \{ -\tfrac{1}{6} q^2(\eta_f^2 + 1) + m_f^2 \}$$

$$-2M_Z^2(M_Z^4 + 2M_Z^2 M_W^2 - 4M_W^4) - \tfrac{1}{3} q^2(M_Z^4 - 2M_Z^2 M_W^2 - 18M_W^4) \Bigg] C_{UV}$$

$$+ \frac{\alpha}{8\pi M_W^2(M_Z^2 - M_W^2)} \Bigg[\sum_{f} M_Z^4 \{(\eta_f^2 + 1) q^2 F(m_f, m_f, q) - m_f^2 F_0(m_f, m_f, q)\}$$

$$-\tfrac{1}{3} q^2(M_Z^4 - 2M_Z^2 M_W^2 + 4M_W^4) + 2M_W^2(M_Z^4 - 4M_Z^2 M_W^2 + 16M_W^4) \ln M_W$$

$$+ M_Z^4(M_Z^2 \ln M_Z + m_\phi^2 \ln m_\phi) - 10M_W^4 q^2 F_0(M_W, M_W, q)$$

$$+ (M_Z^4 - 4M_Z^2 M_W^2 + 24M_W^4) q^2 F(M_W, M_W, q)$$

$$+ M_W^2(3M_Z^4 - 4M_Z^2 M_W^2 - 16M_W^4) F_0(M_W, M_W, q)$$

$$+M_Z^4\{2M_Z^2F_0(m_\phi, M_Z, q)-M_Z^2F_1(m_\phi, M_Z, q)+q^2F(m_\phi, M_Z, q)\}$$

$$-m_\phi^2M_Z^4F_1(M_Z, m_\phi, q)\Big], \tag{3.2}$$

where $\sum_f$ denotes the sum on all flavors and colors, and

$$\eta_f \equiv 2\left\{T_f^3-2Q_f\left(1-\frac{M_W^2}{M_Z^2}\right)\right\}, \quad C_{UV} \equiv \frac{1}{\varepsilon}-\gamma_E+\ln 4\pi. \tag{3.3}$$

(T_f^3 is the third component of the weak isospin and γ_E is the Euler constant.) The functions F_n ($n = 0, 1, 2$) and F are defined by

$$F_n(M_1, M_2, q) \equiv \int_0^1 x^n \ln\{M_1^2(1-x)+M_2^2x-q^2x(1-x)\}dx,$$

$$F(M_1, M_2, q) \equiv F_1(M_1, M_2, q)-F_2(M_1, M_2, q). \tag{3.4}$$

According to Eq. (2.14), we obtain δM_Z^2 and $Z_{ZZ}^{1/2}$ (see Appendix A.2).

NC. 2. Z-A transition self-energy

Relevant diagrams are shown in Fig. 3.4.

$$\Pi^{ZA}(q^2) = \sum_{n=1}^{8}\Pi_{(U)n}^{ZA}(q^2)+\Pi_C^{ZA}(q^2). \tag{3.5}$$

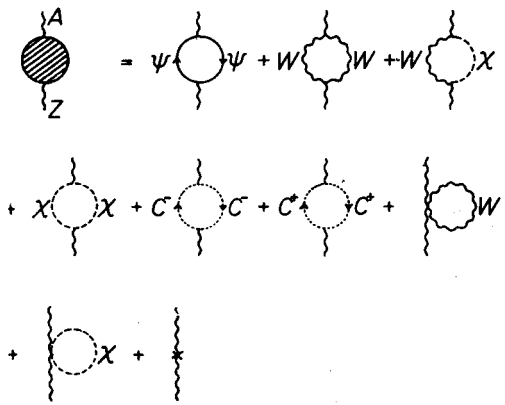

Fig. 3.4. The A–Z transition self-energy

Here

$$\sum_{n=1}^{8}\Pi_{(U)n}^{ZA}(q^2) = \frac{\alpha M_W}{4\pi\sqrt{M_Z^2-M_W^2}}\left[\left\{\tfrac{1}{6}q^2\left(-\sum_f\zeta_f+\frac{M_Z^2}{M_W^2}+18\right)+2M_Z^2\right\}C_{UV}\right.$$

$$-2(M_Z^2-8M_W^2)\ln M_W-(M_Z^2+8M_W^2)F_0(M_W, M_W, q)$$

$$+q^2\left\{\sum_f \zeta_f F(m_f, m_f, q)-\frac{M_Z^2-12M_W^2}{M_W^2}F(M_W, M_W, q)\right.$$

$$\left.-5F_0(M_W, M_W, q)+\frac{M_Z^2-4M_W^2}{6M_W^2}\right\}\Bigg], \tag{3.6}$$

and

$$\zeta_f \equiv \frac{4M_Z^2}{M_W^2}Q_f\left\{T_f^3-2Q_f\left(1-\frac{M_W^2}{M_Z^2}\right)\right\}. \tag{3.7}$$

$Z_{AZ}^{1/2}$ and $Z_{ZA}^{1/2}$ are determined by Eq. (2.14).

By similar computations, we get the remaining renormalization constants δM_W^2, $Z_{L,R}^e$ and Z_L^ν, and Y is fixed through the eeA vertex, the calculations of which are almost the same as those of the eeZ vertex explained below.

NC. 3. eeZ vertex

Relevant graphs are in Fig. 3.5.

$$\Gamma_\alpha^{eeZ}(p_e', p_e) = \sum_{n=1}^{4}\Gamma_{(U)n\alpha}^{eeZ}(p_e', p_e)+\Gamma_{C\alpha}^{eeZ}, \tag{3.8}$$

where $\Gamma_{C\alpha}^{eeZ}$ is the counterterm.

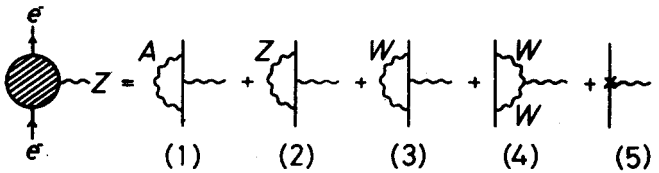

Fig. 3.5. The eeZ vertex diagrams

The first term is somewhat complicated:

$$\Gamma_{(U)1\alpha}^{eeZ}(p_e', p_e) = \frac{e^3}{64\pi^2 M_W\sqrt{M_Z^2-M_W^2}}$$

$$\times\left[(3M_Z^2-4M_W^2)\left\{F(q^2)\gamma_\alpha+G(q^2)\frac{(p_e'+p_e)_\alpha}{2m_e}\right\}\right.$$

$$\left.+M_Z^2\left\{F_5(q^2)\gamma_\alpha\gamma_5+G_5(q^2)\frac{(p_e'-p_e)_\alpha}{2m_e}\gamma_5\right\}\right]. \tag{3.9a}$$

In this equation,

$$F(q^2) = C_{UV}-2\ln m_e+\frac{3}{a}\ln\frac{1+a}{1-a}$$

$$-\frac{1+a^2}{a}\left\{\tfrac{1}{2}\ln\frac{4}{1-a^2}\ln\frac{1+a}{1-a}-2\ln\frac{\lambda}{m_e}\ln\frac{1+a}{1-a}-\phi(a)\right\},$$

$$G(q^2)=-\frac{1-a^2}{a}\ln\frac{1+a}{1-a},$$

$$F_5(q^2)=C_{UV}-2\ln m_e+\frac{1+2a^2}{a}\ln\frac{1+a}{1-a}$$

$$-\frac{1+a^2}{a}\left\{\tfrac{1}{6}\ln\frac{4}{1-a^2}\ln\frac{1+a}{1-a}-2\ln\frac{\lambda}{m_e}\ln\frac{1+a}{1-a}-\phi(a)\right\},$$

$$G_5(q^2)=\frac{1-a^2}{a^2}\left\{\frac{1+2a^2}{a}\ln\frac{1+a}{1-a}-2\right\}, \tag{3.9b}$$

where

$$\phi(a)\equiv Sp\left(\frac{1+a}{2}\right)-Sp\left(\frac{1-a}{2}\right),$$

$$\left(a\equiv\sqrt{\frac{-q^2}{-q^2+4m_e^2}}\right)$$

and

$$Sp(x)\equiv-\int_0^x\frac{1}{t}\ln(1-t)dt \text{ (the Spence function).}$$

On the other hand, the remaining parts become very simple thanks to the approximation of neglecting $q^2/M_{W,Z}^2$ and $m_{e,\mu}/M_{W,Z}$ in comparison with $O(1)$ quantities:

$$\sum_{n=2}^{4}\Gamma^{eeZ}_{(U)n\alpha}(p'_e,p_e)=\frac{e^3M_Z^2}{64\pi^2(M_Z^2-M_W^2)\sqrt{M_Z^2-M_W^2}}$$

$$\times\left[\frac{-M_Z^4}{16M_W^3}(C_{UV}-\tfrac{1}{2}-2\ln M_Z)\gamma_\alpha\{(3\xi+\xi^3)-(1+3\xi^2)\gamma_5\}\right.$$

$$\left.+\left\{\frac{M_Z^2}{2M_W}(C_{UV}-\tfrac{1}{2}-2\ln M_W)-M_W(3C_{UV}-\tfrac{1}{2}-6\ln M_W)\right\}\gamma_\alpha(1-\gamma_5)\right], \tag{3.9c}$$

$$\left(\xi\equiv\frac{4M_W^2-3M_Z^2}{M_Z^2}\right)$$

$$\Gamma^{eeZ}_{C\alpha}=-eZ_{AZ}^{1/2}\gamma_\alpha$$

$$-\frac{eM_Z^2}{4M_W\sqrt{M_Z^2-M_W^2}}\left\{Y+\frac{M_Z^2-2M_W^2}{2(M_Z^2-M_W^2)}\left(\frac{\delta M_Z^2}{M_Z^2}-\frac{\delta M_W^2}{M_W^2}\right)+Z_{ZZ}^{1/2}+Z_L^e\right\}\gamma_\alpha(1-\gamma_5)$$

$$+\frac{e}{M_W}\sqrt{M_Z^2-M_W^2}\,\gamma_\alpha\left\{Y+\frac{M_Z^2}{2(M_Z^2-M_W^2)}\left(\frac{\delta M_Z^2}{M_Z^2}-\frac{\delta M_W^2}{M_W^2}\right)+Z_{ZZ}^{1/2}+\frac{Z_L^e+Z_R^e}{2}-\frac{Z_L^e-Z_R^e}{2}\gamma_5\right\}. \tag{3.9d}$$

NC. 4. ννZ and ννA vertices

Fig. 3.6 and Fig. 3.7 show the relevant diagrams.

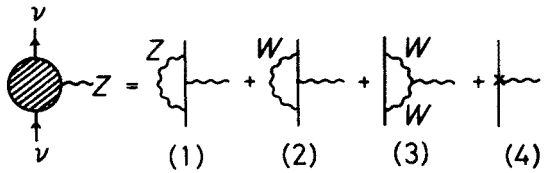

Fig. 3.6. The ννZ vertex diagrams

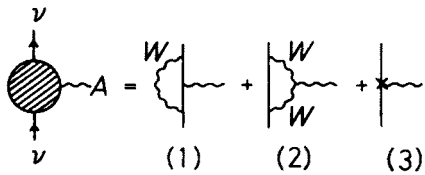

Fig. 3.7. The ννA vertex diagrams

$$\Gamma_\alpha^{\nu\nu Z}(p'_\nu, p_\nu)=\sum_{n=1}^{3}\Gamma_{(U)n\alpha}^{\nu\nu Z}(p'_\nu, p_\nu)+\Gamma_{C\alpha}^{\nu\nu Z}, \tag{3.10}$$

$$\sum_{n=1}^{3}\Gamma_{(U)n\alpha}^{\nu\nu Z}(p'_\nu, p_\nu)$$

$$=\frac{e^3M_Z^2}{64\pi^2(M_Z^2-M_W^2)\sqrt{M_Z^2-M_W^2}}\left\{\frac{(M_Z^2+M_W^2)^2+7M_W^4}{4M_W^3}C_{UV}-\frac{M_Z^4}{4M_W^3}(\tfrac{1}{2}+2\ln M_Z)\right.$$

$$\left.-\frac{M_Z^2-2M_W^2}{2M_W}(\tfrac{1}{2}+2\ln M_W)-M_W(\tfrac{1}{2}+6\ln M_W)\right\}\gamma_\alpha(1-\gamma_5), \tag{3.11a}$$

$$\Gamma_{C\alpha}^{\nu\nu Z}=\frac{eM_Z^2}{4M_W\sqrt{M_Z^2-M_W^2}}\left\{Y+\frac{M_Z^2-2M_W^2}{2(M_Z^2-M_W^2)}\left(\frac{\delta M_Z^2}{M_Z^2}-\frac{\delta M_W^2}{M_W^2}\right)+Z_{ZZ}^{1/2}+Z_L^\nu\right\}\gamma_\alpha(1-\gamma_5). \tag{3.11b}$$

$$\Gamma_\alpha^{\nu\nu A}(p'_\nu, p_\nu)=\sum_{n=1}^{2}\Gamma_{(U)n\alpha}^{\nu\nu A}(p'_\nu, p_\nu)+\Gamma_{C\alpha}^{\nu\nu A}, \tag{3.12}$$

$$\sum_{n=1}^{2} \Gamma^{\nu\nu A}_{(U)n\alpha}(p'_\nu, p_\nu)$$

$$= \frac{e^2 M_Z^2}{96\pi^2(M_Z^2 - M_W^2)}\left[3C_{UV} - 6\ln M_W - \frac{q^2}{M_W^2}\{1 + 2\ln M_W - 6F(m_\mu, m_\mu, q)\}\right]\gamma_\alpha(1-\gamma_5), \tag{3.13a}$$

where q^2/M_W^2 terms must be maintained in connection with the $1/q^2$ term in the photon propagator. The counterterm is

$$\Gamma^{\nu\nu A}_{C\alpha} = \frac{eM_Z^2}{4M_W\sqrt{M_Z^2 - M_W^2}} Z_{ZA}^{1/2}\gamma_\alpha(1-\gamma_5). \tag{3.13b}$$

NC. 5. Box diagrams

The four point functions (Figs 3.1 (7)–(9)) have no divergences, and include $W^\pm$ and Z internal lines, so the result is very simple.

$$A(p'_e, p'_\nu; p_e, p_\nu)_{(7)+(8)+(9)} = \frac{\alpha^2 M_Z^4}{64 M_W^4 (M_Z^2 - M_W^2)^2}\bar{u}_\nu\gamma^\alpha(1-\gamma_5)u_\nu$$

$$\times \bar{u}_e\gamma_\alpha\left\{(28M_W^2 - 9M_Z^2) - \left(15M_Z^2 - 20M_W^2 + \frac{24M_W^4}{M_Z^2}\right)\gamma_5\right\}u_e. \tag{3.14}$$

Collecting the results, we obtain the one-loop-corrected amplitude $\mathscr{A}(\nu e \to \nu e)$ in the following form:

$$\mathscr{A}(\nu e \to \nu e) = \bar{u}_e(p'_e)\left[\gamma^\alpha\{A(q^2) + B(q^2)\gamma_5\} + C(q^2)\frac{(p'_e + p_e)^\alpha}{2m_e}\right]u_e(p_e)$$

$$\times \bar{u}_\nu(p'_\nu)\gamma_\alpha(1-\gamma_5)u_\nu(p_\nu). \tag{3.15}$$

The cross-section is

$$\frac{d\sigma}{dt} = \frac{1}{2\pi}\left[|A - \xi B|^2 + |A + \xi B|^2\left(\frac{u - m_e^2}{s - m_e^2}\right)^2 + 2(|A|^2 - |B|^2)\frac{m_e^2 t}{(s-m_e^2)^2}\right.$$

$$\left. + 4\,\mathrm{Re}\,AC^*\left\{1 + \frac{st}{(s-m_e^2)^2}\right\}\right]. \tag{3.16}$$

($\xi = +1$ for $\nu e \to \nu e$ and $\xi = -1$ for $\bar{\nu}e \to \bar{\nu}e$)

Charged current processes

We need the following renormalization constants:

$$\delta M_W^2,\ \delta M_Z^2,\ Z_W,\ Z_L^l (l = e, \mu),\ Z_L^\nu \text{ and } Y.$$

Among them, Z_W is an only constant which did not appear in the neutral current processes. (Z_L^μ is obtained from Z_L^e by changing m_e to m_μ.) It is determined through the $W^\pm$ self-

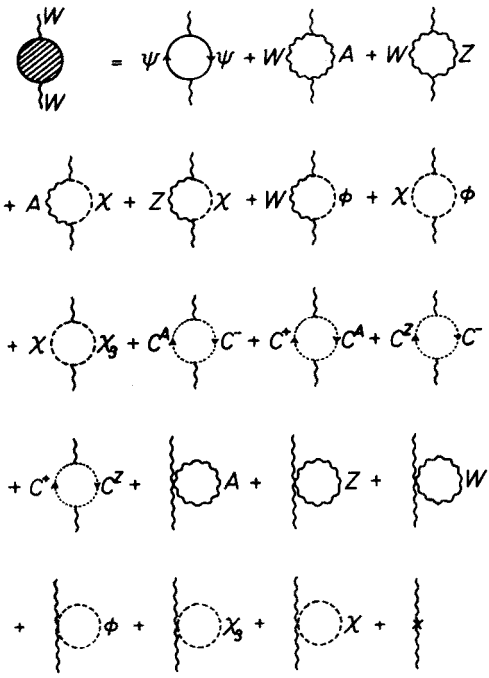

Fig. 3.8. The $W^{\pm}$ boson self-energy. $C^{\pm}$, C^{A} and C^{Z} represent the FP ghosts

-energy explicitly shown in the following. (The $W^{\pm}$ self-energy is a main part of calculations of the charged current processes. So, I explain it here although it was already used in the N.C. processes to fix δM_W^2.)

CC. 1. W boson self-energy

$$\Pi^{W}(q^2) = \sum_{n=1}^{18} \Pi^{W}_{(U)n}(q^2) + \Pi^{W}_{C}(q^2). \tag{3.17}$$

where

$$\sum_{n=1}^{18} \Pi^{W}_{(U)n}(q^2) = \frac{\alpha M_Z^2}{8\pi(M_Z^2 - M_W^2)} \left\{ \sum_{(I,i)} |U_{Ii}|^2 (m_I^2 + m_i^2 - \tfrac{2}{3} q^2) - 2(M_Z^2 - 2M_W^2) + \tfrac{19}{3} q^2 \right\} C_{UV}$$

$$+ \frac{\alpha}{8\pi(M_Z^2 - M_W^2)} \Bigg[2M_Z^2 \sum_{(I,i)} |U_{Ii}|^2 \{ 2q^2 F(m_I, m_i, q)$$

$$- m_i^2 F_1(m_I, m_i, q) - m_I^2 F_1(m_i, m_I, q) \}$$

$$- M_Z^2 \{ q^2 - 14M_W^2 \ln M_W - (12M_W^2 + M_Z^2) \ln M_Z - m_\phi^2 \ln m_\phi \}$$

$$+ (2M_Z^4 - 5M_Z^2 M_W^2 - 14M_W^4) F_0(M_W, M_Z, q)$$

$$- 10M_W^2 q^2 F_0(M_W, M_Z, q) - (M_Z^4 + 15M_Z^2 M_W^2 - 16M_W^4) F_1(M_W, M_Z, q)$$

$$+(M_Z^2+20M_W^2)q^2F(M_W, M_Z, q)$$
$$-2(M_Z^2-M_W^2)\{7M_W^2F_0(M_W, \lambda, q)+5q^2F_0(M_W, \lambda, q)$$
$$-8M_W^2F_1(M_W, \lambda, q)-10q^2F(M_W, \lambda, q)\}$$
$$-m_\phi^2M_Z^2\{F_0(m_\phi, M_W, q)-F_1(m_\phi, M_W, q)\}$$
$$+M_Z^2M_W^2\{2F_0(m_\phi, M_W, q)-F_1(m_\phi, M_W, q)\}+M_Z^2q^2F(m_\phi, M_W, q)\Big]. \tag{3.18}$$

Relevant graphs are shown in Fig. 3.8. (In the actual calculations. I will take only the Cabibbo angle part of U_{Ii} into account.) According to Eq. (2.14), δM_W^2 and Z_W are determined. Now all of the necessary renormalization constants have been fixed.

CC. 2. νlW vertex (l = e, μ)

$$\Gamma_\alpha^{\nu lW}(p_\nu', p_l) = \sum_{n=1}^{4} \Gamma_{(U)n\alpha}^{\nu lW}(p_\nu', p_l)+\Gamma_{C\alpha}^{\nu lW}, \tag{3.19}$$

where

$$\sum_{n=1}^{4} \Gamma_{(U)n\alpha}^{\nu lW}(p_\nu', p_l)$$
$$= \frac{e^3M_Z^3(M_Z^2+10M_W^2)}{128\pi^2M_W^2(M_Z^2-M_W^2)\sqrt{2(M_Z^2-M_W^2)}}\, C_{UV}$$
$$+\frac{e^3M_Z}{64\pi^2\sqrt{2(M_Z^2-M_W^2)}}$$
$$\times\Big[5-12\ln M_W+\frac{M_W^2}{(M_Z^2-M_W^2)^2}\{5(M_Z^2-M_W^2)-12(M_Z^2\ln M_Z-M_W^2\ln M_W)\}$$
$$-\frac{M_Z^2(M_Z^2-2M_W^2)}{4M_W^2(M_Z^2-M_W^2)}(1+4\ln M_Z)\Big]\gamma_\alpha(1-\gamma_5), \tag{3.20a}$$

$$\Gamma_{C\alpha}^{\nu lW} = \frac{eM_Z}{4\sqrt{2(M_Z^2-M_W^2)}}$$
$$\times\left\{\frac{-M_W^2}{M_Z^2-M_W^2}\left(\frac{\delta M_Z^2}{M_Z^2}-\frac{\delta M_W^2}{M_W^2}\right)+2Y+Z_L^l+Z_L^\nu+Z_W\right\}\gamma_\alpha(1-\gamma_5). \tag{3.20b}$$

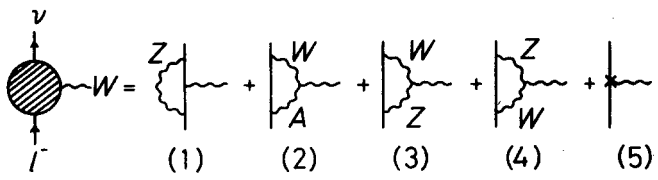

Fig. 3.9. The νlW$^\pm$ vertex diagrams (l = e or μ)

CC. 3. Box diagrams

The contributions of the box diagrams except for the photon exchange graph are rather easily evaluated (Figs 3.2 (5), (6), (8) and (9)) due to the same reason as in NC.5.

$$A(p'_\mu, p'_\nu; p_e, p_\nu)_{(5)+(6)+(8)+(9)}$$
$$= \frac{\alpha^2 M_Z^2(3M_Z^4-6M_Z^2M_W^2-2M_W^4)}{8M_W^2(M_Z^2-M_W^2)^3} \ln\frac{M_Z}{M_W}\, \bar{u}_\mu\gamma^\alpha(1-\gamma_5)u_\nu \cdot \bar{u}_\nu\gamma_\alpha(1-\gamma_5)u_e. \quad (3.21a)$$

On the other hand, it is not so easy to carry out the loop integral of the graph Fig. 3.2 (7). By applying the Fierz transformation due to a technical reason, the result is given as

$$\bar{u}_\mu(p'_\mu)\,[A(u)\gamma^\alpha(1-\gamma_5)+B(u)\gamma^\alpha(1+\gamma_5)+C(u)\,(1-\gamma_5)\,(p_e)^\alpha$$
$$+D(u)\,(1+\gamma_5)\,(p_e)^\alpha]u_e(p_e)\cdot\bar{u}_\nu(p'_\nu)\gamma_\alpha(1-\gamma_5)u_\nu(p_\nu), \quad (3.21b)$$

$$A(u) = G\left[\frac{m_\mu^2+m_e^2-u}{R}\left\{2RT\ln\frac{R}{2\lambda^2}+\ln\left(\frac{4m_\mu^2}{-u}\right)\ln\frac{m_e^2-m_\mu^2-u+R}{2m_\mu\sqrt{-u}}\right.\right.$$
$$\left.+\ln\left(\frac{4m_e^2}{-u}\right)\ln\frac{m_\mu^2-m_e^2-u+R}{2m_e\sqrt{-u}}-\phi\left(\frac{R}{-u},\frac{m_\mu^2-m_e^2}{-u}\right)\right\}$$
$$\left.-\tfrac{1}{2}-\ln\frac{M_W^2}{m_\mu m_e}-\frac{m_\mu^2-m_e^2}{u}\ln\frac{m_\mu}{m_e}+\frac{(m_\mu^2-m_e^2)^2-4(m_\mu^2+m_e^2)u+3u^2}{u}T\right],$$

$$B(u) = -4m_\mu m_e GT,$$

$$C(u) = \frac{2m_\mu G}{u}\left\{\ln\frac{m_\mu}{m_e}+(m_e^2-m_\mu^2+u)T\right\},$$

$$D(u) = \frac{2m_e G}{u}\left\{\ln\frac{m_e}{m_\mu}+(m_\mu^2-m_e^2+u)T\right\},$$

$$G \equiv \frac{\alpha^2 M_Z^2}{8M_W^2(M_Z^2-M_W^2)}, \quad R \equiv \sqrt{(m_\mu^2-m_e^2+u)^2-4m_\mu^2 u}, \quad T \equiv \frac{1}{R}\ln\frac{m_\mu^2+m_e^2-u+R}{2m_\mu m_e},$$

$$\phi(a,b) \equiv Sp\left(\frac{a+1+b}{2a}\right)-Sp\left(\frac{a-1+b}{2a}\right)+Sp\left(\frac{a+1-b}{2a}\right)-Sp\left(\frac{a-1-b}{2a}\right). \quad (3.21c)$$

Collecting all the parts, we obtain the one-loop-corrected amplitude the form of which is same as Eq. (3.21b), where all the contributions except for the photon exchange box diagram are collected into the term A. Then, the cross-section is written as

$$\frac{d\sigma}{dt} = \frac{2}{\pi(s-m_e^2)^2}\,[|A|^2(s-m_\mu^2)\,(s-m_e^2)+2m_\mu m_e\,\mathrm{Re}\,(AB^*)u$$
$$+(m_\mu^2 m_e^2-st)\,\mathrm{Re}\,A^*(m_\mu C+m_e D)]. \quad (3.22)$$

So far, I have calculated the amplitude for $\nu_\mu e \to \mu\nu_e$, but the amplitude for μ decay can be obtained by the same functions and the width is calculated as

$$\frac{d^2\Gamma}{dE_e d\cos\theta} = \frac{|\boldsymbol{p}_e|\,(m_\mu^2+m_e^2-2m_\mu E_e)^2}{4\pi^3(m_\mu-E_e+|\boldsymbol{p}_e|\cos\theta)^4}$$

$$\times\,[|A|^2\{(m_\mu^2+m_e^2)E_e+(m_\mu^2-m_e^2)\,|\boldsymbol{p}_e|\cos\theta-2m_\mu m_e^2\}$$

$$-2m_e\,\mathrm{Re}\,A^*B(m_\mu-E_e+|\boldsymbol{p}_e|\cos\theta)^2+m_\mu\,\mathrm{Re}\,A^*(m_\mu C+m_e D)\,|\boldsymbol{p}_e|^2\sin^2\theta] \qquad (3.23)$$

(θ is the angle between e and $\bar{\nu}_e$).

Now we have obtained the UV convergent quantities. Since the electroweak theory is known to be renormalizable, it is not surprising that all the UV divergences, C_{UV}, completely cancel out in final results. But in actual computations, such cancellation seems sometimes even miraculous since we have to deal with a lot of terms together. (As a matter of fact, Aoki and I almost invented a new notion "spontaneous breakdown of renormalizability" (!?) when we failed to eliminate UV divergences due to some miscalculations.) It may be one of the reasons why many people feel that gauge theories are correct for describing fundamental interactions.

3.2. IR, CL divergences and real photon emission

As a next step in practical calculations, we have to treat the other divergences, i.e., the infrared (IR) and the collinear (CL) divergences. As was mentioned, the latter one is not a real divergence in the present calculations. However, we still have to eliminate it in relation to actual experimental setup, which will be explained later.

First, let us see why such divergences appear. In the diagram of Fig. 3.10, the denominator of the fermion propagator is

$$m^2-(p+k)^2 = -2|\boldsymbol{k}|\,(\sqrt{\boldsymbol{p}^2+m^2}-|\boldsymbol{p}|\cos\theta). \qquad (3.24)$$

Apparently it becomes zero when $|\boldsymbol{k}|$ goes to zero (IR div.), or when θ takes vanishing value if $m = 0$ (CL div.). Such divergences appear also in diagrams with virtual photon correction in connection with the value of loop momentum. It is easily understood that their origin is the emission of real or virtual photon.

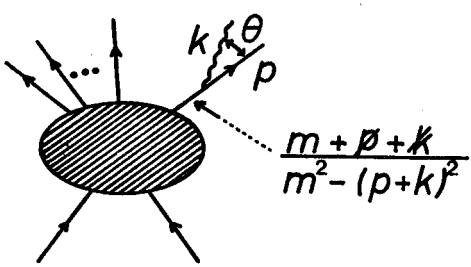

Fig. 3.10. An example of a real photon emission process. k and p express the momenta of the photon and the fermion respectively, and θ is the angle between $\boldsymbol{k}$ and $\boldsymbol{p}$

The well-known Kinoshita-Lee-Nauenberg theorem [21] says that real and virtual photon emissions give opposite sign contributions, and they completely cancel out with each other. So, if we define the cross-section, e.g., of $\nu e \to \nu e$ as a sum of those of $\nu e \to \nu e$ and $\nu e \to \nu e\gamma$ (Fig. 3.11), we can get a result free from those divergences. From the experimental point of view, such a definition means that photons with momentum smaller than some value or emitted almost collinearly to charged particle cannot be detected. (The actual conditions depend on the resolution of experimental apparatus.)

Let us proceed to concrete calculations for these real photon emissions. Strictly speaking, there is a little difference between $\nu(\bar{\nu})e \to \nu(\bar{\nu})e\gamma$ and $\nu e \to \mu\nu\gamma$ (or $\mu \to e\nu\bar{\nu}\gamma$). That is, three graphs contribute for the latter (see Figs. 3.12 and 3.13). Actually, however, the diagram of Fig. 3.13 (2) has no contribution to the IR divergence and gives only very small magnitude, so we can neglect it safely. Then, simultaneous treatments become possible for both processes.

Practical evaluations of those diagrams' contributions become very easy if we restrict the emitted photon energy to be much smaller than that of e or μ (the soft photon approximation). That is, by expressing the tree cross-section of $\nu(\bar{\nu})e \to \nu(\bar{\nu})e$ or $\nu e \to \mu\nu$ as $d\sigma_0$, the cross-section of $\nu(\bar{\nu})e \to \nu(\bar{\nu})e\gamma$ or $\nu e \to \mu\nu\gamma$, $d\sigma^{\text{soft}}$, can be represented as

$$d\sigma^{\text{soft}} = -\frac{\alpha}{4\pi^2}\int\frac{d^3k}{E_\gamma}\left(\frac{p_e}{kp_e}-\frac{p_l'}{kp_l'}\right)^2\cdot d\sigma_0 \quad (l = e, \mu). \tag{3.25}$$

(A similar formula holds, of course, for $\mu \to e\nu\bar{\nu}$.)

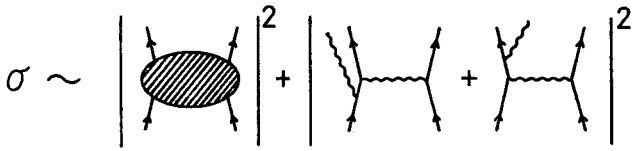

Fig. 3.11

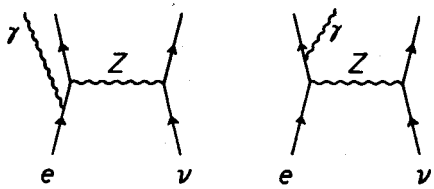

Fig. 3.12. The real photon emission in the $\nu_\mu(\bar{\nu}_\mu)e \to \nu_\mu(\bar{\nu}_\mu)e$ process

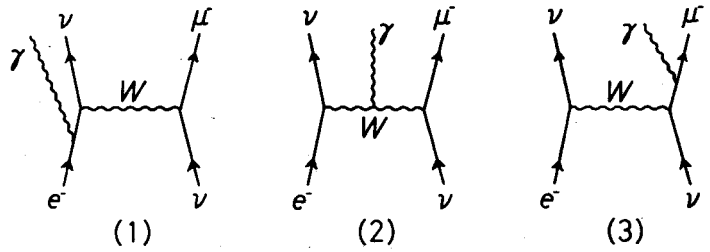

Fig. 3.13. The real photon emission in the process $\nu_\mu e \to \mu\nu_e$ ($\mu \to e\nu_\mu\bar{\nu}_e$)

Effects of the addition $d\sigma^{\text{soft}}$ to the one-loop-corrected cross-section $d\sigma^{(1)}(\text{ve} \to \text{vl})$ are as follows:

(*i*) The IR divergence term $\ln \lambda$ in $d\sigma^{(1)}$ is replaced by $\ln(2\omega)$, where ω is the maximum of the emitted photon energy (so we may set $\lambda = 0$ safely), and

(*ii*) A term, $2C_{\text{soft}} d\sigma_0$ (the ω and λ independent part of the above integral in the Lab. frame) is added, where

$$C_{\text{soft}} = \frac{\alpha}{2\pi}\left[1 + \frac{E_1'}{|\boldsymbol{p}_1'|}\ln\left(\frac{E_1'+|\boldsymbol{p}_1'|}{m_1}\right)\left\{1-2\ln 2-\ln\frac{|\boldsymbol{p}_1'|^2}{m_1(E_1'+|\boldsymbol{p}_1'|)}\right\}\right.$$
$$\left. - \frac{E_1'}{|\boldsymbol{p}_1'|}\left\{\frac{\pi^2}{6} - Sp\left(\frac{E_1'-|\boldsymbol{p}_1'|}{E_1'+|\boldsymbol{p}_1'|}\right)\right\}\right]. \tag{3.26}$$

As a result we obtain the UV and IR convergent quantities (cross-sections or decay-width). However the (approximate) CL divergence still remains and produces extremely large EM corrections, which is theoretically rather peculiar. Furthermore, this situation and the constraint $\omega \ll E_1$ (they are not independent to each other) are both experimentally quite unrealistic since they correspond to a statement that we can distinguish $\text{ve} \to \text{vl}$ and $\text{ve} \to \text{vl}\gamma$ as long as $E_\gamma \geqslant \omega$ even if γ is emitted collinearly to l or E_γ is much smaller than E_1.

Therefore, in order to derive more realistic results, we must estimate the contributions of Figs. 3.12 and 3.13 (except for 3.13 (2)) without taking the soft photon approximation (hard photon effects [8, 9, 22, 23]). After some tedious computations, we obtain

$$\sum_{\text{spin}} |\mathscr{M}(\text{ve} \to \text{vl}\gamma)|^2 = -64G_{\text{H}}^2\left[\frac{1}{(kp_1')^2}[(m_1^2-kp_1')\{(1+\xi)^2(p_e p_\nu)(p_1'p_\nu'+kp_\nu')\right.$$
$$+(1-\xi)^2(p_e p_\nu')(p_1'p_\nu+kp_\nu)\}+(1-\xi^2)m_1^3 m_e(p_\nu p_\nu')]$$
$$-\frac{1}{(kp_1')(kp_e)}[2(1+\xi^2)\{(kp_e)(p_1'p_\nu)(p_1'p_\nu')-(kp_1')(p_e p_\nu)(p_e p_\nu')\}$$
$$+2(1-\xi^2)m_1 m_e\{(p_1'p_e)(p_\nu p_\nu')+(kp_\nu)(kp_\nu')\}$$
$$+(1+\xi)^2(p_1'p_e)\{2(p_1'p_\nu')(p_e p_\nu)-(kp_\nu)(p_1'p_\nu')+(kp_\nu')(p_e p_\nu)\}$$
$$+(1-\xi)^2(p_1'p_e)\{2(p_1'p_\nu)(p_e p_\nu')-(kp_\nu')(p_1'p_\nu)+(kp_\nu)(p_e p_\nu')\}]$$
$$+\frac{1}{(kp_e)^2}[(m_e^2+kp_e)\{(1+\xi)^2(p_1'p_\nu')(p_e p_\nu-kp_\nu)+(1-\xi)^2(p_1'p_\nu)(p_e p_\nu'-kp_\nu')\}$$
$$\left.+(1-\xi^2)m_1 m_e^3(p_\nu p_\nu')]\right], \tag{3.27}$$

where k is the photon momentum, and

$$G_H = \frac{-e^3 M_Z^2}{16 M_W^2 (M_Z^2 - M_W^2)}, \quad \xi = \frac{4M_W^2 - 3M_Z^2}{M_Z^2} \quad \text{for} \quad ve \to ve\gamma$$

$$G_H = \frac{e^3 M_Z^2}{8 M_W^2 (M_Z^2 - M_W^2)}, \quad \xi = 1 \quad \text{for} \quad ve \to \mu\nu\gamma.$$

The formula for $\bar{v}e \to \bar{v}e\gamma$ is obtained by changing $\xi \to -\xi$, and the one for $\mu \to e\nu\bar{\nu}\gamma$ is also derived by modifying the above formula slightly.

Taking these contributions into account, we have the UV, IR and CL convergent quantities. Of course, the hard photon effects also depend on actual experimental conditions, but we can now consider any condition. Numerical analysis based on these results is carried out in the next Section.

4. O(α) corrections for physical quantities

The main purpose of this Section is to determine the values of the renormalized parameters and make numerical analysis, but it is useful to clarify first the meaning of the "electromagnetic (EM)" part and the "weak" part in the whole electroweak radiative corrections since they are sometimes discussed separately.

4.1. EM and weak corrections

In principle, the electromagnetic correction is defined by the diagrams which include photonic correction only.

Its meaning is quite clear in the case of the neutral current processes (Fig. 4.1 plus the corresponding counterterms). The diagram in Fig. 4.1 has not only the UV divergence but also includes the IR and CL ones, which are eliminated by considering the real photon emission, Fig. 3.12. At one-loop order, the latters do not appear in the other diagrams. So the weak part, which is defined by the sum of the remaining diagrams, is free from the IR and CL divergences, and consequently does not depend on experimental conditions.

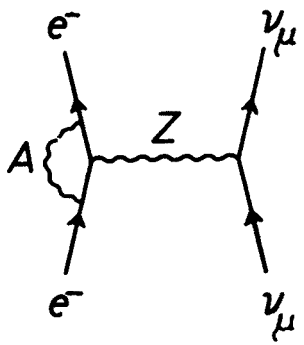

Fig. 4.1. The purely electromagnetic one-loop correction for the process $\nu_\mu(\bar{\nu}_\mu)e \to \nu_\mu(\bar{\nu}_\mu)e$

On the other hand, the situation for the charged current processes is rather complicated. The diagram which corresponds to Fig. 4.1 is Fig. 3.2 (7). This is UV convergent but includes the IR and CL divergences. However they cannot be eliminated even after adding the real photon emission effects, which can be explicitly seen in the results in Sect. 3. Therefore we have to find another way.

The traditional one, which I adopt in the following, is to define the EM part by the photonic correction to the four-fermion interaction (Fig. 4.2 plus the counterterms). In this scheme, the real photon emissions are given by Fig. 4.3. By representing the radiative

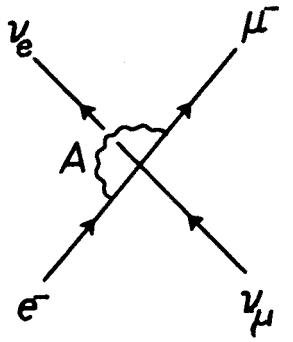

Fig. 4.2. The purely electromagnetic one-loop correction for the process $\nu_\mu e \to \mu\nu_e(\mu \to e\nu_\mu\bar{\nu}_e)$ in the framework of the four-fermion interaction

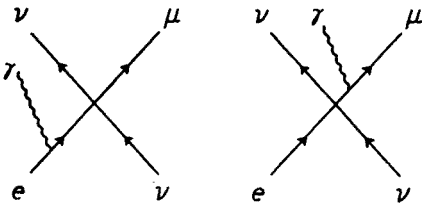

Fig. 4.3

correction from this EM part as Δ_{EM} and the whole one-loop (electroweak) correction as Δ, the weak correction Δ_{W} is defined as

$$\Delta_{\mathrm{W}} = \Delta - \Delta_{\mathrm{EM}}. \tag{4.1}$$

Let us express the amplitudes including the whole one-loop effects and only the weak effects as $\mathscr{A}$ and $\mathscr{A}_{\mathrm{W}}$ respectively, and those corresponding to Fig. 4.2 (plus counterterms) and to Fig. 3.2 (7) as $\mathscr{A}_{\mathrm{EM}}$ and $\mathscr{A}_{\mathrm{Box}}$ respectively. After some calculations, we can find the following relation:

$$\mathscr{A}_{\mathrm{EM}} = \mathscr{A}_{\mathrm{Box}} + \tfrac{1}{2}\left\{Z^{\mathrm{e}} + Z^{\mu} - \frac{\alpha}{4\pi}(1 + 4\ln M_{\mathrm{W}})\right\}\mathscr{A}_0, \tag{4.2a}$$

where

$$Z^{\mathrm{l}}(\mathrm{l} = \mathrm{e}, \mu) = -\frac{\alpha}{2\pi}\left\{2 - \ln m_{\mathrm{l}} + 2\ln\left(\frac{\lambda}{m_{\mathrm{l}}}\right)\right\}, \tag{4.2b}$$

and $\mathscr{A}_0$ is the tree amplitude of $\nu_\mu e \to \mu\nu_e$. On the other hand, it is easy to see

$$\mathscr{A} = [\ldots + \mathscr{A}_{\text{Box}} + \ldots + \tfrac{1}{2}(Z_L^e + Z_L^\mu)\mathscr{A}_0 + \ldots], \tag{4.3}$$

and the UV convergent part (C_{UV} independent part) of Z_L^1 is

$$Z_L^1 = Z^1 + \frac{\alpha}{16\pi M_W^2(M_Z^2 - M_W^2)}\{M_Z^2 M_W^2(1+4\ln M_W) + (M_Z^2 - 2M_W^2)^2(\tfrac{1}{2} + 2\ln M_Z)\}. \tag{4.4}$$

(See Appendix A.2.) Then, the IR (which exists only in $\mathscr{A}_{\text{Box}}$ and Z^1) and the CL (included only in $\mathscr{A}_{\text{Box}}$) divergences disappear in $\mathscr{A}_W \equiv \mathscr{A} - \mathscr{A}_{EM}$.

Therefore, also in this case, $\mathscr{A}_W$ does not depend on actual experimental setup.

4.2. Numerical results

We are now ready to determine the values of the parameters. At present, we have experimental information of α and various masses (except for m_t and m_ϕ), so we can directly substitute them (I express them as α^{exp}, M_W^{exp}, ...) into the corresponding parameters thanks to the on-mass-shell renormalization. Then, a radiative correction to a cross-section σ is evaluated as

$$\Delta = (\sigma^{(1)} - \sigma^{(0)})/\sigma^{(0)}, \tag{4.5}$$

where $\sigma^{(1)}$ and $\sigma^{(0)}$ are the one-loop-corrected and the tree level cross-sections respectively:

$$\sigma^{(1),(0)} = \sigma^{(1),(0)}(\alpha^{\text{exp}}, M_W^{\text{exp}}, M_Z^{\text{exp}}, m_f^{\text{exp}}, m_\phi^{\text{exp}}).$$

Here we have of course to use some assumed values of m_t and m_ϕ, but the results do not depend sensitively on these values unless they are extremely large as will be shown in Sect. 5.2.

However we want to see how the success of the theory at tree level is affected by the inclusion of higher order effects, and the tree analyses have been done with the following input data,

$$\alpha^{\text{exp}}(= 1/137.036), \quad G_F^{\text{exp}}(= (1.16632 \pm 0.00002) \times 10^{-5}\ \text{GeV}^{-2}),$$
$$\sin^2\theta_W^{\text{exp}}(\sim 0.23) \quad (\text{and } m_f^{\text{exp}}, m_\phi^{\text{exp}}). \tag{4.6}$$

Therefore we should use them also in one-loop analysis. In this case, our task is to determine the values of M_W and M_Z from G_F^{exp}, $\sin^2\theta_W^{\text{exp}}$ and others.

Let us assume that $\sin^2\theta_W^{\text{exp}}$ is obtained from the data of $\nu_\mu e \to \nu_\mu e$. Then, expressing the amplitudes of $\nu_\mu e \to \nu_\mu e$ and $\mu \to e\nu_\mu\bar{\nu}_e$ as

$$\mathscr{A}(\nu e \to \nu e) = \bar{u}_e\gamma^\alpha\{A^{\text{NC}}(q^2) + B^{\text{NC}}(q^2)\gamma_5\}u_e \cdot \bar{u}_\nu\gamma_\alpha(1-\gamma_5)u_\nu, \tag{4.7a}$$

$$\mathscr{A}(\mu \to e\nu\bar{\nu}) = A^{\text{CC}}(q^2)\bar{u}_e\gamma^\alpha(1-\gamma_5)v_{\bar{\nu}} \cdot \bar{u}_\nu\gamma_\alpha(1-\gamma_5)u_\nu, \tag{4.7b}$$

we obtain the following simultaneous equations[3]

$$\frac{1}{4}\left\{1+\frac{A^{\mathrm{NC}}(q^2)}{B^{\mathrm{NC}}(q^2)}\right\}\Big|_{q^2=\langle q^2\rangle^{\mathrm{exp}}}\left(=1-\frac{M_{\mathrm{W}}^2}{M_{\mathrm{Z}}^2}\text{ at tree level}\right)=\sin^2\theta_{\mathrm{W}}^{\mathrm{exp}}, \tag{4.8a}[4]$$

$$A^{\mathrm{CC}}(0)\left(=\frac{-\pi\alpha M_{\mathrm{Z}}^2}{2M_{\mathrm{W}}^2(M_{\mathrm{Z}}^2-M_{\mathrm{W}}^2)}\text{ at tree level}\right)=-\frac{G_{\mathrm{F}}^{\mathrm{exp}}}{\sqrt{2}}. \tag{4.8b}$$

Here it should be mentioned that $\mathscr{M}_{\mathrm{W}}$ (ve → ve) and $\mathscr{M}_{\mathrm{W}}$ ($\mu \to \mathrm{e}\nu\bar{\nu}$) are used as the one-loop-corrected amplitudes (otherwise the right-hand-sides of Eq. (4.7) become more complicated (see Eqs. (3.15) and (3.21b)). The reason is as follows:
In the case of the muon decay, for instance, the following equation is used [9, 22] when expressing the actual data Γ^{exp} in terms of G_{F},

$$\Gamma^{\mathrm{exp}}=\frac{G_{\mathrm{F}}^2 m_\mu^5}{192\pi^3}\left(1-\frac{8m_{\mathrm{e}}^2}{m_\mu^2}\right)\left(1+\frac{\alpha^{\mathrm{exp}}}{2\pi}\left(\tfrac{25}{4}-\pi^2\right)\right). \tag{4.9}$$

That is, the $O(\alpha)$ EM effects have already been taken into account at this step. Therefore, the equation (4.8b) at one-loop level is equivalent to

$$\Gamma^{(\mathrm{W})}=\Gamma^{\mathrm{exp}}\cdot(1-\Delta_{\mathrm{EM}}), \tag{4.10}$$

($\Gamma^{(\mathrm{W})}$: μ decay width with the weak correction only) except for the neglected q^2 dependence, and further equivalent to

$$\Gamma^{(1)}(=\Gamma^{(\mathrm{W})}\cdot(1+\Delta_{\mathrm{EM}}))=\Gamma^{\mathrm{exp}}, \tag{4.11}$$

which is consistent with Eq. (1.6) in Sect. 1.

Let us take this opportunity to give some comments on another important parameter ϱ. Apparently, it is quite misleading to define ϱ by the equation

$$\varrho=M_{\mathrm{W}}^2/(M_{\mathrm{Z}}^2\cos^2\theta_{\mathrm{W}}),$$

since one of the simplest definitions of θ_{W} is

$$\cos\theta_{\mathrm{W}}\equiv M_{\mathrm{W}}/M_{\mathrm{Z}}.$$

We should use the equation

$$\varrho\equiv 2B^{\mathrm{NC}}(0)/A^{\mathrm{CC}}(0)\quad(=1\text{ at tree level}). \tag{4.12}$$

I think it is much clearer to deal with the electroweak effects as a whole, but the EM and the weak parts have, so far, often discussed separately as was shown in the above. One reason is that the one-loop EM correction to the four-fermion interaction $\mu \to \mathrm{e}\nu\bar{\nu}$

[3] Strictly speaking, we should compare $\langle\sigma^{\nu\mathrm{e}\to\nu\mathrm{e}}\rangle\equiv\int\phi(E_\nu)\sigma^{\nu\mathrm{e}\to\nu\mathrm{e}}(E_\nu)dE_\nu$ (ϕ: neutrino energy spectrum) and Γ (the μ decay width) with the corresponding data, but the resultant difference is small.

[4] In the actual computations, I have used the ratio $R_\nu\equiv\sigma(\bar{\nu}\mathrm{e}\to\bar{\nu}\mathrm{e})/\sigma(\nu\mathrm{e}\to\nu\mathrm{e})$ (see Appendix A.1), but I show this equation here in order to clarify the meaning of "$\sin^2\theta_{\mathrm{W}}^{\mathrm{exp}}$".

had been known to be finite [22] and consequently G_F had been determined through Eq. (4.9) before the electroweak theory was proposed. And, in fact, this theory was constructed to reproduce the four-fermion coupling effectively concerning the low energy charged current phenomena. Another reason is: many people consider that the weak part is just important for precise tests of the theory since it was impossible to get any well-defined weak correction when weak phenomena were being studied in the framework of the above-mentioned four-fermion interaction. But such a separate treatment may come to be unpopular in future.

Anyway, let us determine the values of M_W and M_Z from Eq. (4.8). First, using the tree level formulas on the left-hand-sides, we obtain the well-known results

$$M_W^{(0)}\left(=\sqrt{\frac{\pi\alpha^{\exp}}{\sqrt{2}\,G_F^{\exp}\sin^2\theta_W^{\exp}}}=\frac{37.2813}{|\sin\theta_W^{\exp}|}\right)\sim 77\ \text{GeV}, \tag{4.13a}$$

$$M_Z^{(0)}\,(=M_W^{(0)}/\cos\theta_W^{\exp})\sim 88\ \text{GeV}, \tag{4.13b}$$

where "(0)" means the lowest order approximation. (These values correspond to $\sin^2\theta_W^{\exp}=0.2344$.)

Similarly, we compute $M_W^{(1)}$ and $M_Z^{(1)}$ using the formulas in Sect. 3. In practical computations, the perturbative method is often used by setting $M_{W,Z}^{(1)}=M_{W,Z}^{(0)}+\Delta M_{W,Z}$. The results are

$$M_W^{(1)}\simeq 79.25\ \text{GeV},\quad M_Z^{(1)}\simeq 90.64\ \text{GeV}. \tag{4.14}$$

(We may also solve the equations directly by computer calculations as $M_W^{(1)}\simeq 79.17$ GeV and $M_Z^{(1)}\simeq 90.54$ GeV [5]. The differences are interpreted as parts of higher order effects.)

The most part of the above large one-loop effects is due to the coexistence of $\alpha\ln m_f$ terms and $\alpha\ln M_{W,Z}$ terms in the results. (The formers exist in Y, Π^{ZA} and $\Gamma_\alpha^{\nu\nu A}$). In Sect. 3 I gave formulas with $\mu=1$, where μ is the parameter appearing in the dimensional regularization. But, of course, the final results do not depend on μ, so setting $\mu=M_W$ we can find approximate formulas easily from Y, Π^{ZA} and $\Gamma_\alpha^{\nu\nu A}$ as follows:

$$M_W^{(1)}\simeq M_W^{(0)}\left\{1+\frac{\alpha^{\exp}}{6\pi\sin^2\theta_W^{\exp}}\left(\ln\frac{m_\mu^{\exp}}{M_W^{(0)}}-\sum_f Q_f T_f^3\ln\frac{m_f^{\exp}}{M_W^{(0)}}\right)\right\}, \tag{4.15a}$$

$$M_Z^{(1)}\simeq M_Z^{(0)}\left\{1-\frac{\alpha^{\exp}}{3\pi}\tan^2\theta_W^{\exp}\sum_f Q_f^2\ln\frac{m_f^{\exp}}{M_W^{(0)}}\right.$$

$$\left.+\frac{\alpha^{\exp}}{6\pi}\left(\frac{1}{\sin^2\theta_W^{\exp}}-\frac{1}{\cos^2\theta_W^{\exp}}\right)\left(\ln\frac{m_\mu^{\exp}}{M_W^{(0)}}-\sum_f Q_f T_f^3\ln\frac{m_f^{\exp}}{M_W^{(0)}}\right)\right\}. \tag{4.15b}$$

(Here I have set $\langle q^2\rangle=0$ for simplicity.)

Now all the parameters have been fixed, and we can calculate $O(\alpha)$ radiative corrections for various quantities. For example, weak one-loop correction to a cross-section σ is

$$\Delta_W = \frac{\sigma^{(1)}(\alpha^{exp}, M^{(1)}_{W,Z}, m_f^{exp}, m_\phi^{exp}) - \sigma^{(0)}(\alpha^{exp}, M^{(0)}_{W,Z}, m_f^{exp}, m_\phi^{exp})}{\sigma^{(0)}(\alpha^{exp}, M^{(0)}_{W,Z}, m_f^{exp}, m_\phi^{exp})}. \tag{4.16}$$

instead of Eq. (4.5). Here, of course, $\sigma^{(1)}$ is a quantity with the weak correction only. On the other hand, the EM correction essentially depends only on α and estimated in the same way as in QED.

I show the EM and weak corrections for the processes studied so far in Table 4.1, where I have used the following values for the other parameters; $m_\nu = 0$, $m_e = 5.11 \times 10^{-4}$, $m_\mu = 1.057 \times 10^{-1}$, $m_\tau = 1.782$, $m_u = m_d = m_s = 0.1$, $m_c = 1.5$, $m_b = 4.7$, $m_t = 30$ and $m_\phi = 10$ (in GeV unit) and $\sin^2\theta_C$ (the Cabibbo angle) $= 0.0562$. (Δ_W for μ decay is exactly zero since I have used the condition $\Gamma^{(W)} = \Gamma^{(0)}$.) In the table, Δ_{EM}^{soft} means the

TABLE 4.1

The $O(\alpha)$ corrections for the tree cross-sections of $\nu_\mu e \to \nu_\mu e$, $\bar\nu_\mu e \to \bar\nu_\mu e$, $\nu_\mu e \to \mu\nu_e$ and the width of $\mu \to e\nu_\mu\bar\nu_e$. E_ν^{Lab} means the laboratory neutrino (or antineutrino) energy in GeV unit. Δ_W, Δ_{EM}^{soft} and Δ_{EM} represent the weak correction, the EM correction with the soft photon effect only, and the EM correction with the real (soft and hard) photon effects

E_ν^{Lab} (GeV)	Δ_W	Δ_{EM}^{soft} (ω = 1 keV)	Δ_{EM}^{soft} (ω = 100 keV)	Δ_{EM}
		$\nu_\mu e \to \nu_\mu e$		
1	0.86(%)	−25.7	−12.6	−1.4
10^2	0.89	−56.2	−33.3	−2.1
10^4	0.99	−96.6	−63.8	−2.9
		$\bar\nu_\mu e \to \bar\nu_\mu e$		
1	0.87	−25.3	−12.4	−1.4
10^2	0.84	−55.8	−33.0	−2.1
10^4	0.74	−96.1	−63.5	−2.9
		$\nu_\mu e \to \mu\nu_e$		
15	0.00	−21.7	−12.1	−4.5
10^2	0.00	−30.6	−18.2	−2.4
10^4	−0.01	−64.2	−42.5	−2.9
		$\mu \to e\nu_\mu\bar\nu_e$		
	0 (input)	−17.9	−9.5	−0.4

EM correction with the effects of the soft photon only, the maximum energy of which is ω. Therefore, Δ_{EM}^{soft} still includes the (approximate) CL divergence. The corresponding erms are, for example in $\nu_\mu e \to \nu_\mu e$,

$$\tfrac{1}{2}\ln\frac{4}{1-a^2}\ln\frac{1+a}{1-a}+2\ln m_e \ln\frac{1+a}{1-a} \quad \left(a\equiv\sqrt{\frac{-q^2}{-q^2+4m_e^2}}\right) \text{ in Eq. (3.9b).}$$

Apparently these terms diverge in the limit of $|q^2| \to \infty$, and it is the origin of the extremely large value Δ_{EM}^{soft}.

As was explained in Sect. 3.2, Δ_{EM} depends on an actual experimental condition, and values given in Table 4.1 are those obtained by integrating the photon momentum to all over the kinematically allowed region in the phase space. That is, the present values of Δ_{EM} correspond to a situation in which any event with a photon in the final state is taken into account for estimating the cross-section of $\nu e \to \nu l$ (or the width of $\mu \to e\nu\bar{\nu}$) regardless of the size of the photon momentum. (Of course, we can estimate the value of Δ_{EM} corresponding to another situation. For such studies, see [9].)

Anyway, we find that the radiative corrections Δ_W and Δ_{EM} are very small, so the success of the theory is not affected. It is certainly a confirmation of the theory beyond tree approximation, but is quite a passive one. Then, is it possible to make clearer test of the higher order effects? This is the subject of the next Section.

5. Experimental verification of loop effects

One possibility of making a clean (positive) test of loop effects is to use the masses of $W^\pm$ and Z bosons. Equations (4.13) and (4.14) are "theoretical predictions" for M_W and M_Z, and should be compared with M_W^{exp} and M_Z^{exp}. If $M_{W,Z}^{(1)}$ are more favored than $M_{W,Z}^{(0)}$ definitely, it will be the first clear confirmation of the higher order effects. This seems to be possible in the near future since the $O(\alpha)$ effects, $\Delta M_{W,Z} \equiv M_{W,Z}^{(1)} - M_{W,Z}^{(0)}$ are large, and we will obtain $M_{W,Z}^{exp}$ with an accuracy of 0.1–0.2 GeV.

Actually, however, we need a further device to realize this possibility since we cannot draw a definite conclusion from the mere comparison of $M_{W,Z}^{(1),(0)}$ with $M_{W,Z}^{exp}$ due to the following reason: The results (4.14) have been derived from the fixed $M_{W,Z}^{(0)}$ (Eq. (4.13)), but the actual $M_{W,Z}^{(0)}$ have non-negligible uncertainties ($M_W^{(0)} = 77.9 \pm 1.7$ GeV and $M_Z^{(0)} = 88.8 \pm 1.4$ GeV) because the present data on θ_W include a rather large error, at least $\sim 5\%$ ($\sin^2\theta_W^{exp} = 0.229 \pm 0.010$ [24])[5]. Therefore $M_{W,Z}^{(0)}$ and $M_{W,Z}^{(1)}$ have an overlapping allowed region (Fig. 5.1), and consequently the one-loop effects become totally unclear. According to Bailin (in [4]), it is important to calculate radiative corrections when both of the followings are satisfied:

(*i*) There is a theory which makes a precise prediction of the zeroth order effects;
(*ii*) There are experiments which are precise enough to be sensitive to $O(\alpha)$ effects.

---

[5] Strictly speaking, we must not use this value since it is an average value of those obtained mainly in νN reactions while we are considering $\nu e \to \nu e$. If we use the data from $\nu e \to \nu e$ only, ambiguities become much larger.

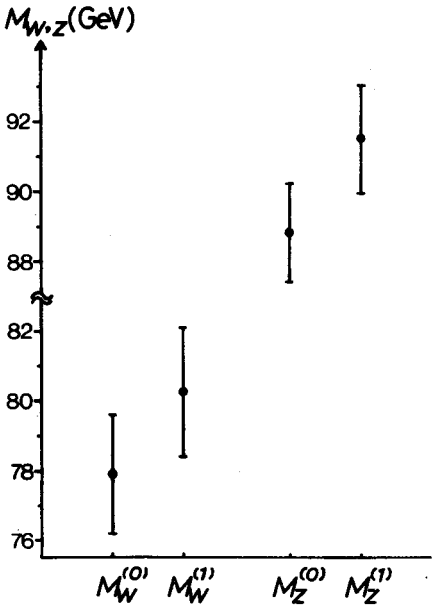

Fig. 5.1. The tree and one-loop calculations of M_W and M_Z. The ambiguities come from the error in θ_W^{exp} ($\sin^2\theta_W^{exp} = 0.229 \pm 0.010$)

The calculations of $M_{W,Z}$ do not satisfy the first criterion, though the second will become satisfied in the near future. (It will not be so easy to get much precise θ_W^{exp} since it is mainly measured in neutrino experiments.)

In order to improve this situation, let us make analysis without θ_W^{exp}, i.e., with Eq. (4.8b) only. Consequently, we obtain the interrelation between M_W and M_Z instead of the separate predictions for them [10, 20, 25, 26]. Let us call it the $M_W - M_Z$ relation. In other words, we take a new scheme in which, e.g., M_W (and other quantities) are computed by the input data α^{exp}, M_Z^{exp}, G_F^{exp}, m_f^{exp} and m_ϕ^{exp}.

First (in Sect. 5.1), I explain this relation assuming that all particles are relatively light ($\lesssim 100$ GeV), and subsequently study the effects expected when some of the particles (m_t or m_ϕ) are very heavy.

5.1. $M_W - M_Z$ relation and light particle effects

In order to derive a form of the $M_W - M_Z$ relation more convenient for actual calculations, I divide A^{CC} in Eq. (4.7b) into two parts: the tree part A_0 and the one-loop correction A_1,

$$A^{CC} = A_0(\alpha, M_W, M_Z) + A_1(\alpha, M_W, M_Z, m_f, m_\phi).$$

The tree relation is obtained by using A_0 (see Eq. (4.8b)) only as

$$M_W^{(0)} = M_Z\left[\tfrac{1}{2}\left(1+\sqrt{1-\frac{2\sqrt{2}\,\pi\alpha}{M_Z^2 G_F}}\right)\right]^{1/2}. \tag{5.1}$$

(Here and in the following, I sometimes neglect the superscript "exp" for simplicity.) The one-loop-corrected relation is derived from

$$A_0(\alpha, M_W, M_Z)+A_1(\alpha, M_W, M_Z, m_f, m_\phi) = -\frac{G_F}{\sqrt{2}}. \tag{5.2}$$

This equation can be solved perturbatively by setting the solution as $M_W^{(1)} = M_W^{(0)}+\Delta M_W$ and neglecting ΔM_W in A_1:

$$M_W^{(1)} = \left[M_W+\frac{M_W^3(M_Z^2-M_W^2)^2}{\pi\alpha M_Z^2(2M_W^2-M_Z^2)}A_1(\alpha, M_W, M_Z, m_f, m_\phi)\right]\Bigg|_{M_W=M_W^{(0)}}. \tag{5.3}$$

(As was explained before, we may solve the above equation numerically, but the resultant difference is in this case very small, at most 0.01 GeV in the absolute value of $M_W^{(1)}$ [10].)

In Table 5.1 is given the numerical M_W-M_Z relation. We can find large one-loop effects, $|M_W^{(1)}-M_W^{(0)}| \sim 1$ GeV, which mainly come from the large logarithmic terms as was shown in Sect. 4.2. Picking up only the log terms, we obtain an approximate formula:

$$M_W^{(1)} = \left[M_W+\frac{\alpha}{3\pi}\left\{\frac{M_W(M_Z^2-M_W^2)}{2M_W^2-M_Z^2}\sum_f Q_f^2 \ln\left(\frac{m_f}{M_W}\right)\right\}\right]_{M_W=M_W^{(0)}}. \tag{5.4}$$

Here readers may have a question: In the preceding calculations, we have observed that $M_{W,Z}^{(1)}$ are larger than $M_{W,Z}^{(0)}$. Then, why is $M_W^{(1)}$ smaller than $M_W^{(0)}$ in the present analysis? The answer is obtained from Fig. 5.2, in which I have drawn two kinds of curves on the M_W-M_Z plane. That is, one is a set of the curves corresponding to the present M_W-M_Z relation (curves (*1*), there the dashed and solid curves are the tree level and the one-loop-corrected relations respectively) and the other is another M_W-M_Z relation derived from a condition

$$\frac{1}{4}\left\{1+\frac{A^{NC}(q^2)}{B^{NC}(q^2)}\right\} = \sin^2\theta_W^{exp},$$

TABLE 5.1

The numerical M_W-M_Z relation. As for the quark and the Higgs masses, I have used $m_u = m_d = m_s = 0.1$ GeV, $m_c = 1.5$ GeV, $m_b = 4.7$ GeV, $m_t = 30$ GeV and $m_\phi = 10$ GeV

M_Z	$M_W^{(0)}$	$M_W^{(1)}$
90.0 (GeV)	79.49	78.49
92.0	81.92	80.99
94.0	84.31	83.43

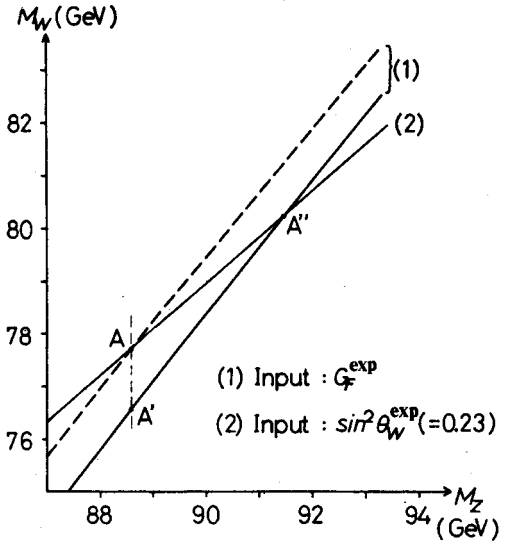

Fig. 5.2. Weak boson mass relations. The curves (*1*) are the relations obtained from G_F^{exp} (the dashed one is for tree level and the solid one for one-loop level), and the curve (*2*) is the one obtained from $\sin^2\theta_W^{exp}$ instead of G_F^{exp}

only (curve (*2*), there I have used a value $\sin^2\theta_W = 0.23$ and assumed $q^2 = 0$). In the latter case, I have drawn only one curve since the tree and the one-loop-corrected curves almost overlap, which can be confirmed by making an approximate formula as follows.

$$M_W^{(1)\prime} = \left[M_W + \frac{\alpha M_Z^2}{6\pi M_W} \left\{ \ln \frac{m_\mu}{M_W} - \sum_f Q_f T_f^3 \ln \frac{m_f}{M_W} \right.\right.$$

$$\left.\left. + 2 \sin^2\theta_W^{exp} \sum_f Q_f^2 \ln \frac{m_f}{M_W} \right\} \right]_{M_W = M_W{}^{(0)\prime}}, \tag{5.5a}$$

and

$$M_W^{(0)\prime} = M_Z \cos\theta_W^{exp}. \tag{5.5b}$$

(I have used the notation $M_W{}'$ in order to distinguish it from the relation Eq. (5.3).) That is, due to the opposite sign contributions of the log terms, $|M_W^{(1)\prime} - M_W^{(0)\prime}|$ becomes very small, e.g., ~ 0.17 GeV for $M_Z = 90$ GeV. If we use both conditions simultaneously as in Sect. 4.2, the separate predictions for M_W and M_Z are obtained. The tree predictions are given by the point A, and the one-loop-corrected ones are A'' in Fig. 5.2. Apparently, $M_{W,Z}^{(1)} > M_{W,Z}^{(0)}$. On the other hand, I have made use of only one condition (Eq. (4.8b)) here, and computed M_W for fixed M_Z. Therefore, the prediction for M_W moves from A to A' by the inclusion of the loop effects. That is, $M_W^{(1)} < M_W^{(0)}$ in this case.

Anyway, the large one-loop effects make us expect that a clean test of the theory may be possible. However, we should make further studies since

° I have neglected the strong interaction (QCD) effects in the quark loop diagrams,
° The large one-loop effects indicate that the two (and higher) loop effects may be also non-negligible, and
° There may be ambiguities from quark and Higgs masses.
Let us examine these problems.
(*i*) Light quark mass and QCD effects

As was already explained, the main origin of the large one-loop correction is the coexistence of $\alpha \ln m_f$ and $\alpha \ln M_{W,Z}$ terms, and their combinations are especially significant in the case of light fermions; e, μ, u, d and s. The $\alpha \ln m_f$ terms are included in Y (see Eq. (A.7)). This Y is in the counterterm for $\nu lW^{\pm}$ vertex, and is determined by $Z_{AA}^{1/2}$ and several other renormalization constants through the on-mass-shell condition for eeA vertex. That is, the above $\alpha \ln m_f$ terms come from the fermion loop corrections to the photon self-energy.

Concerning the light quark sector of them, I have used the values $m_u = m_d = m_s = 0.1$ GeV, but we cannot measure the quark masses directly, i.e., we do not know if these values are correct ones. For example, $M_W^{(1)}$ decreases about 0.1 GeV if current quark masses $m_u = 4.2 \times 10^{-3}$ GeV, $m_d = 7.5 \times 10^{-3}$ GeV and $m_s = 0.15$ GeV (and $m_c = 1.15$ GeV) are used [10]. So, we must recognize that the $M_W - M_Z$ relation in Table 5.1 includes light quark mass ambiguities.

Furthermore, these calculations have been done in the framework of the free quark picture, i.e., the QCD effects have not been taken into account. Non-negligible terms may have been dropped through this approximation since $Z_{AA}^{1/2}$ is derived from $\Pi_{(U)}^{A'}(q^2)$ at $q^2 = 0$ where the QCD effects are not necessarily small.

Therefore, we have to find a way to estimate the size of quark contributions to the photon self-energy unambiguously. One of the most effective approaches is to use the data of the total cross-section $\sigma(e^+e^- \to \gamma^* \to \text{hadrons})$ with a help of the following dispersion relation [20, 26a, 27–29],

$$\mathrm{Re}\,[\pi^A(s)]_{\text{quark}} = \frac{s}{4\pi^2\alpha} \int_{4m_\pi^2}^{\infty} \frac{\sigma(s'; e^+e^- \to \text{hadrons})}{s' - s}\, ds'. \tag{5.6}$$

$$(\Pi^A(s) \equiv -s\pi^A(s))$$

Then the quark contribution to $Z_{AA}^{1/2}$ can be estimated as follows by taking some large s (e.g., M_W^2) where the QCD effects are un mportant ($\alpha_{QCD}(M_W^2) \simeq 0.12$ [30]):

$$\begin{aligned}[Z_{AA}^{1/2}]_{\text{quark}} &= -\tfrac{1}{2}\,[\pi_{(U)}^A(0)]_{\text{quark}} \\ &= \tfrac{1}{2}\,\mathrm{Re}\,[\pi^A(s) - \pi_{(U)}^A(s)]_{\text{quark}}.\end{aligned} \tag{5.7}$$

That is, the second term can be evaluated in the framework of the free quark picture, while the first important term depends (through Eq. (5.6)) only on the experimental data. Of course we have to use some values for quark masses to calculate the second term, but they

are unimportant:

$$\mathrm{Re}\,[\pi^{\mathrm{A}}_{(\mathrm{U})}(M_{\mathrm{W}}^2)]_{\mathrm{quark}} = \frac{\alpha}{3\pi}\sum_{\mathrm{q}} Q_{\mathrm{q}}^2 \left\{ C_{\mathrm{UV}} + \tfrac{5}{3} + O\left(\frac{m_{\mathrm{q}}^2}{M_{\mathrm{W}}^2}\right)\right\}.$$

As a matter of fact, $m_{\mathrm{u}} = m_{\mathrm{d}} = m_{\mathrm{s}} = 0.1$ GeV have been derived by fitting the free quark model to the numerical result obtained from the above procedure [31], i.e., they are "effective" quark masses which include the full QCD effects.

This problem on the quark loop contributions has recently been studied also by other non-perturbative methods [32]. By taking these investigations into account together, the corresponding ambiguity in $M_{\mathrm{W}}^{(1)}$ is estimated to be, at most, $\sim \pm 0.05$ GeV.

(ii) Higher loop effects

We are now allowed to make calculations in the framework of free quark picture with "effective" masses concerning the strong interaction effects. Then, as a next study, we should examine the electroweak two (and higher) loop contributions.

The bulk of the large one-loop effects comes from $\alpha \ln (m/M)$ term, so let us estimate the size of $[\alpha \ln (m/M)]^n$ $(n \geqslant 2)$ contributions. Fortunately we are familiar with such log corrections in perturbation calculations of QCD, GUT etc., and have a well-founded technique to treat them: the renormalization group technique [33, 34]. Since it is not possible to give detailed explanations of this technique here, I only give the result: By the inclusion of $[\alpha^n \ln^n]$ effects, $\frac{\alpha}{3\pi}\sum_{\mathrm{f}} Q_{\mathrm{f}}^2 \ln \frac{m}{M}$ in Eq. (5.4) is replaced by $\frac{1}{2}\left\{1 - \frac{\alpha(M)}{\alpha}\right\}$ as [11],

$$M_{\mathrm{W}} = \left[M_{\mathrm{W}} + \frac{M_{\mathrm{W}}(M_{\mathrm{Z}}^2 - M_{\mathrm{W}}^2)}{2(2M_{\mathrm{W}}^2 - M_{\mathrm{Z}}^2)}\left(1 - \frac{\alpha(M_{\mathrm{W}})}{\alpha}\right)\right]_{M_{\mathrm{W}} = M_{\mathrm{W}}^{(0)}}, \tag{5.8a}$$

where $\alpha(\mu)$ is the running coupling constant

$$\alpha(\mu) = \alpha\left\{1 + \frac{2\alpha}{3\pi}\sum_{\mathrm{f}} Q_{\mathrm{f}}^2 \ln\left(\frac{m_{\mathrm{f}}}{\mu}\right)\right\}^{-1}. \tag{5.8b}$$

Consequently, the value of the $\mathrm{W}^{\pm}$ boson mass decreases slightly; $\simeq 0.07$ GeV. In addition, $O(\alpha^2 \ln)$ contributions have been found negligible in [35].

In Table 5.2, I again give numerical results in more detail to show the $O(\alpha)$, $O(\alpha \ln)$ and $O(\alpha + \sum_n \alpha^n \ln^n)$ effects.

TABLE 5.2

$M_{\mathrm{W}}^{(1)}[\alpha]$, $M_{\mathrm{W}}^{(1)}[\alpha + \alpha \ln]$ and $M_{\mathrm{W}}[\alpha + \Sigma\alpha^n \ln^n]$ represent the values with the $O(\alpha)$ (non-leading) effects only, with the full one-loop effects, and with the full one-loop correction plus all the leading logarithmic effects respectively

M_{Z}	$M_{\mathrm{W}}^{(0)}$	$M_{\mathrm{W}}^{(1)}[\alpha]$	$M_{\mathrm{W}}^{(1)}[\alpha + \alpha \ln]$	$M_{\mathrm{W}}[\alpha + \Sigma\alpha^n \ln^n]$
90.0 (GeV)	79.49	79.54	78.49	78.41
92.0	81.92	81.97	80.99	80.92
94.0	84.31	84.35	83.43	83.36

(*iii*) Top quark and Higgs boson mass effects

I have used the value 30 GeV for the top quark mass. If a larger value is used, $M_W^{(1)}$ increases. For example, it increases about 0.2 GeV for a change $m_t = 30$ GeV $\to$ 100 GeV [10]. Of course, this ambiguity disappears if m_t is fixed experimentally as the preliminary UA1 report says [36].

On the other hand, $M_W^{(1)}$ decreases about 0.1 GeV for a change $m_\phi = 10$ GeV $\to$ 100 GeV [10].

Presently inevitable ambiguities are those from the light quark loops and the Higgs mass, and fortunately both of them have been found small compared with the size of the one-loop effects $|M_W^{(1)} - M_W^{(0)}| \simeq 1$ GeV. So we have now obtained the result with quite satisfactory precision[6].

Let us proceed to a more concrete analysis. How precisely must M_W and M_Z be measured for an unambiguous test of the loop effects? This has been assessed in [37], and a theoretically more detailed argument has been given in [38].

Suppose we get data on the Z boson mass as $M_Z = M_Z^{exp} \pm \Delta M_Z^{exp}$. Then, corresponding ambiguity appears in the calculated M_W as

$$M_W^{(n)} = M_W^{(n)}[M_Z^{exp}] \pm \frac{\partial M_W^{(n)}}{\partial M_Z} \Delta M_Z^{exp} \quad (n = 0, 1). \tag{5.9}$$

Since we can expect $M_{W,Z}^{exp} \gg \Delta M_Z^{exp}$, we may set

$$\frac{\partial M_W^{(1)}}{\partial M_Z} \sim \frac{\partial M_W^{(0)}}{\partial M_Z} = \left[\frac{M_W}{M_Z} + \frac{\pi \alpha M_Z}{\sqrt{2}\, G_F M_W (2M_W^2 - M_Z^2)} \right]_{M_W = M_W^{(0)}}. \tag{5.10}$$

Next, let us assume that $W^\pm$ boson mass is determined with an error ΔM_W^{exp}. Then, we can reject (at least) one of the results $M_W^{(0),(1)}$, e.g., at the 68% (95%) confidence level if the following condition is satisfied,

$$|M_W^{(1)}[M_Z^{exp}] - M_W^{(0)}[M_Z^{exp}]| > 2\sigma (4\sigma), \tag{5.11a}$$

where

$$\sigma \equiv \sqrt{\left(\frac{\partial M_W^{(0)}}{\partial M_Z} \right)^2 (\Delta M_Z^{exp})^2 + (\Delta M_W^{exp})^2}, \tag{5.11b}$$

since this assures that there is no region of M_W^{exp} simultaneously belonging to the 68% (95%) confidence territories of $M_W^{(0)}$ and $M_W^{(1)}$. For example, for $M_Z^{exp} = 93$ GeV, ΔM_W^{exp} has to be less than 0.47 GeV (0.21 GeV) for $\Delta M_Z^{exp} = 0.1$ GeV. $(\partial M_W^{(0)}/\partial M_Z \simeq 1.19)$.

This numerical result is interesting since M_W and M_Z will be measured within the error of 0.1–0.2 GeV in the near future. Therefore we will be able to make a clean test of the electroweak theory as a renormalizable field theory by the use of the $M_W - M_Z$ relation.

---

[6] In this lecture, I did not mention an ambiguity from the choice of renormalization scheme since it is considered to be small. Recently, a paper on this problem has appeared [17], in which the scheme dependence of the $M_W - M_Z$ relation is shown to be in fact weak.

Finally some arguments should be made on the meaning of "test of the electroweak higher order effects". As was repeatedly mentioned, $\alpha \ln (m_f/M_W)$ is the major source of the one-loop effects, and it can be expressed very simply by using the running QED coupling constant $\alpha(M_W)$ (see Eq. (5.8)). So, some people assert that it is essentially a pure EM effect, and experimental confirmation of it is insufficient as a test of the electroweak higher order effects. However, it is too much to say, I think, that $\alpha \ln (m/M)$ is a pure EM effect. As I have explained, the pure EM correction to the μ decay width depends only on α, not $\alpha(M_W)$, and the existence of $\alpha(M_W)$ in the result can be properly understood only when the whole electroweak effects are calculated. Of course, it is desirable to avoid such a problem, and it will be possible when the $O(\alpha)$ (not $O(\alpha \ln)$) effects are observed. However, it seems quite difficult since they are very small (see Table 5.2), and comparable with the theoretical ambiguities studied in this subsection.

5.2. Heavy particle search

So far I have assumed that all particles are not so heavy (less than ~ 100 GeV). However, we do not know the value of m_ϕ, and have only preliminary information on m_t [36]. Furthermore there may exist heavy fermions of the fourth, fifth, ... generation. Teherefore, it is interesting to study how the $M_W - M_Z$ relation is affected by particles heavier than 100 GeV.

First, let us give some general remarks on heavy particle effects. Heavy particle effects are suppressed by inverse powers of its mass if the size of the coupling constant in a theory is kept small. This fact is known as the decoupling theorem [34, 39]. In the following, I show a simple example in QED. A fermion (with mass m and charge e) contribution to the photon self-energy $\Pi^{A,\alpha\beta}_{(U)}(q^2)$ is

$$\Pi^{A,\alpha\beta}_{(U)f}(q^2) = -\frac{\alpha}{3\pi}(g^{\alpha\beta}q^2 - q^\alpha q^\beta)$$

$$\times [C_{UV} - 6\int_0^1 dx x(1-x) \ln \{m^2 - q^2 x(1-x)\}]$$

$$\equiv \left(g^{\alpha\beta} - \frac{q^\alpha q^\beta}{q^2}\right) \Pi^A_{(U)f}(q^2), \tag{5.12a}$$

and the corresponding counterterm is

$$\Pi^{A,\alpha\beta}_C = -(g^{\alpha\beta}q^2 - q^\alpha q^\beta) Z_3. \tag{5.12b}$$

According to the on-mass-shell renormalization procedure, we obtain the renormalized one as

$$\Pi^A_f(q^2) = \frac{2\alpha}{\pi} q^2 \int_0^1 dx x(1-x) \ln \left(1 - \frac{q^2}{m^2} x(1-x)\right). \tag{5.13}$$

In the case of $m^2 \gg |q^2|$, this formula becomes

$$\longrightarrow \frac{\alpha}{15\pi} q^2 \left(-\frac{q^2}{m^2}\right)\left\{1+O\left(\frac{q^2}{m^2}\right)\right\},$$

so heavy fermion effect is in fact suppressed.

On the other hand, some couplings are proportional to m_f or m_ϕ in the electroweak theory, so the condition on the size of coupling is not satisfied when we consider the large m_f or m_ϕ limit. Consequently their effects are not necessarily suppressed. Conversely speaking, once $M_{W,Z}$ are precisely determined, we may obtain useful information on unknown heavy particles [12, 13, 29, 40]. This is the reason why studies of heavy particle effects in the $M_W - M_Z$ relation are important.

The m_f and m_ϕ dependence of A^{CC}, from which the $M_W - M_Z$ relation is derived, comes from

a) $W^\pm$ boson self-energy,

b) $\nu l W^\pm (l = e, \mu)$ vertices because the corresponding counterterms include δM_W^2, δM_Z^2, Z_W and Y.

However, a) is not important due to the same reason as the above-mentioned example, and also it is not difficult to confirm that the $m_{f,\phi}$ dependence of Z_W (and Y) is at most logarithmic. On the other hand, the contribution of, e.g., a fermion doublet with masses m_I and m_i to the unrenormalized $W^\pm$ self-energy (except for C_{UV} and the over-all factor) is

$$\Pi^W_{(U)}(q^2) \sim \int_0^1 dx\{m_I^2(1-x)+m_i^2 x-2q^2x(1-x)\} \ln\{m_I^2(1-x)+m_i^2x-q^2x(1-x)\}. \quad (5.14)$$

Remembering that $\delta M_W^2 = -\mathrm{Re}\,\Pi^W_{(U)}(M_W^2)$ (and $\delta M_Z^2 = -\mathrm{Re}\,\Pi^Z_{(U)}(M_Z^2)$), we can recognize that $\delta M^2_{W,Z}$ have the possibility of producing unsuppressed large mass effects. So, I examine $\delta M^2_{W,Z}$ parts in the $\nu l W^\pm$ vertex.

Let us first study heavy fermion effects. $\delta M^2_{W,Z}$ contributions to $A^{CC}(= A_0 + A_1)$ are

$$[A_1(\alpha, M_W, M_Z, m_f, m_\phi)]_{\delta M_{W,Z}^2} = \frac{\pi\alpha M_Z^2}{2(M_Z^2-M_W^2)^2}\left(\frac{\delta M_Z^2}{M_Z^2}-\frac{\delta M_W^2}{M_W^2}\right), \quad (5.15)$$

and m_f^2 dependent parts of $\delta M^2_{W,Z}$ are

$$[\delta M_Z^2]_{m_f^2} = \frac{\alpha M_Z^4 C_{\text{color}}}{8\pi M_W^2(M_Z^2-M_W^2)} m_f^2 \int_0^1 dx \ln\{m_f^2 - M_Z^2 x(1-x)\}$$

$$\longrightarrow \frac{\alpha M_Z^4 C_{\text{color}}}{4\pi M_W^2(M_Z^2-M_W^2)} m_f^2 \ln m_f \quad (m_f \gg M_{W,Z}), \quad (5.16)$$

$$[\delta M_W^2]_{m_f^2} = \frac{\alpha M_Z^2 C_{\text{color}}}{4\pi(M_Z^2-M_W^2)}\left[m_i^2 \int_0^1 dx x \ln\{m_I^2(1-x)+m_i^2x-M_W^2x(1-x)\}\right.$$

$$+m_I^2\int_0^1 dxx\ln\{m_i^2(1-x)+m_I^2x-M_W^2x(1-x)\}\Big]$$

$$\to\frac{\alpha M_Z^2C_{\text{color}}}{4\pi(M_Z^2-M_W^2)}\left(m_i^2\ln m_i+m_I^2\ln m_I-\frac{m_i^2+m_I^2}{4}-\frac{m_i^2m_I^2}{m_I^2-m_i^2}\ln\frac{m_i}{m_I}\right),$$

$$(\text{Case A}: m_I, m_i \gg M_{W,Z}) \tag{5.17a}$$

$$\to\frac{\alpha M_Z^2C_{\text{color}}}{4\pi(M_Z^2-M_W^2)}m_f^2(\ln m_f-\tfrac{1}{4}), \tag{5.17b}$$

$$(\text{Case B}: m_I(m_i)\gg m_i(m_I), M_{W,Z};\quad m_f\equiv\max[m_I, m_i])$$

where $C_{\text{color}}=3$ for quarks and $=1$ for leptons, and the δM_W^2 formula is given for a doublet $(\psi_I, \psi_i)_L$ whose masses are m_I and m_i. If m_t is very large, we have to use Eq. (5.17b). In this case, the m_t^2 dependent part of the M_W-M_Z relation is given as

$$[M_W^{(1)}]_{m_t^2}=\left\{M_W+\frac{3\alpha M_WM_Z^2}{32\pi(M_Z^2-M_W^2)(2M_W^2-M_Z^2)}m_t^2\right\}_{M_W=M_W^{(0)}}. \tag{5.18}$$

We can see that precise measurements of $M_{W,Z}$ will really give us useful information on heavy fermions.

Before making more concrete numerical analysis, I study large m_ϕ effects. In this case, we have to examine some terms independent of $\nu l W^\pm$ vertex too, which I explain later.

First, the m_ϕ^2 dependent parts of $\delta M_{W,Z}^2$ are

$$[\delta M_Z^2]_{m_\phi^2}=\frac{-\alpha M_Z^4}{8\pi M_W^2(M_Z^2-M_W^2)}m_\phi^2\left[\ln m_\phi-\int_0^1 dxx\ln\{m_\phi^2x+M_Z^2(1-x)^2\}\right]$$

$$\to\frac{-\alpha M_Z^4}{32\pi M_W^2(M_Z^2-M_W^2)}\quad m_\phi^2(m_\phi\gg M_{W,Z}), \tag{5.19}$$

$$[\delta M_W^2]_{m_\phi^2}=\frac{-\alpha M_Z^2}{8\pi(M_Z^2-M_W^2)}m_\phi^2\left[\ln m_\phi-\int_0^1 dxx\ln\{m_\phi^2x+M_W^2(1-x)^2\}\right]$$

$$\to\frac{-\alpha M_Z^2}{32\pi(M_Z^2-M_W^2)}\quad m_\phi^2(m_\phi\gg M_{W,Z}). \tag{5.20}$$

As is easily seen, the m_ϕ^2 terms cancel out in the combination $\delta M_Z^2/M_Z^2-\delta M_W^2/M_W^2$. That is, concerning the $\delta M_{W,Z}^2$ parts, we can say that the m_ϕ dependence of the M_W-M_Z relation is weak.

Next, let us explain the above-mentioned additional m_ϕ dependence. It comes from the Nambu-Goldstone boson, χ, exchange which has been neglected in the calculations

in Sect. 3 because of the suppression factor $\sim m_e m_\mu / M_{W,Z}^2$. For example, the $\chi\chi\phi$ vertex is proportional to m_ϕ^2, so the diagram with the $\chi\phi$-loop-corrected χ propagator seems to produce a m_ϕ^4 dependent part! After some explicit calculations, however, we can again find that all m_ϕ^4 and m_ϕ^2 dependent terms completely cancel out (see e.g., [13]), and there remains, at best, $\ln m_\phi$ dependence in the final result[7].

Therefore, now, we can conclude that the role of the Higgs scalar in the $M_W - M_Z$ relation is unimportant unless m_ϕ is extremely large, and the dominant contribution of heavy particles comes from the m_f^2 terms. I show the $M_W^{(1)} - m_t$ curve in Fig. 5.3 for inputs $m_\phi = 10$, 100 and 300 GeV, and $M_Z = 91.6$ GeV [12, 13]. (This seemingly odd value, M_Z, has been taken in order to make the $M_W - M_Z$ relation hold for $M_W = 81$ GeV and $m_t = 150$ GeV as an example.) We can observe that the m_ϕ dependence of the result is in fact weak, and the top quark search will become possible once precise $M_{W,Z}^{exp}$ are obtained.

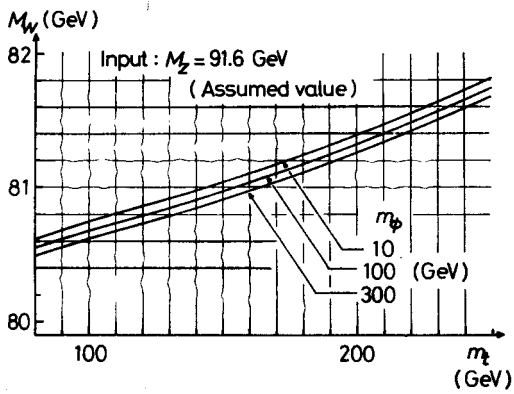

Fig. 5.3. The $M_W - m_t$ plot for assumed values $M_Z = 91.6$ GeV and $m_\phi = 10$, 100 and 300 GeV

So far, a similar analysis has been made through the ϱ-parameter [43, 44]. However, we have at present only an upper bound on m_t ($\lesssim 310$ GeV) [44] due to a non-negligible uncertainty in ϱ^{exp}. Therefore the use of the $M_W - M_Z$ relation will be more effective in the near future[8].

Finally I wish to comment on the usual separate predictions for $M_{W,Z}$ in relation to the heavy fermion search. As an example, I take the frequently referred one [46][9]:

$$\begin{aligned} M_W^{(1)} &= 83.0^{+3.0}_{-2.8}\ \text{GeV}, \\ M_Z^{(1)} &= 93.8^{+2.5}_{-2.4}\ \text{GeV}. \end{aligned} \quad \text{for} \quad m_t = 18\ \text{GeV} \tag{5.21}$$

[7] Such a cancellation is known to occur always in one-loop analysis [41], but it does not hold at more than two-loop order, and perturbation breaks down for $m_\phi \gtrsim$ a few TeV [42].

[8] It should be mentioned that we will not see any interesting effect when $m_I \simeq m_i$, e.g., in the fourth generation even if m_I and $m_i \gg M_{W,Z}$, although such a mass pattern is considered rather unplausible judging from those of the known fermions. One interesting possibility in such a situation is to study processes with external Higgs legs [45].

[9] These values are somewhat different from those of Eq. (4.14). One reason is: the $\nu N \to \nu X$ and the $\nu N \to \mu X$ processes have been used instead of $\nu(\bar{\nu})e \to \nu(\bar{\nu})e$.

If we get experimental data, e.g.,

$$M_W^{exp} = 84.0 \text{ GeV}, \quad M_Z^{exp} = 92.8 \text{ GeV},$$

what can we conclude? At first sight, the agreement of $M_{W,Z}^{(1)}$ and $M_{W,Z}^{exp}$ seems good, and one may conclude naively that the higher order effects have been clearly observed. Actually, however, this is not true: The difference $M_Z^{exp} - M_W^{exp} = 8.8$ GeV is too small to be consistently fitted by the theory if $m_t = 18$ GeV. As a matter of fact, we need $m_t \simeq 325$ GeV in order to make the $M_W - M_Z$ relation hold at one-loop level for $M_W = 84.0$ GeV and $M_Z = 92.8$ GeV in the framework of three generations and $m_\phi = 10$ GeV.

The reason why such a confusion occurs is apparent: The ambiguities in Eq. (5.21) come from only one origin, i.e., $\Delta \sin^2 \theta_W^{exp}$, and are correlated with each other. So, we are not allowed to consider a situation $M_W = 83.0 + 1.0$ GeV and $M_Z = 93.8 - 1.0$ GeV. Such a trivial point is, of course, known by the authors, and I have no mind to find fault with their work. My aim here is to stress that heavy fermion effects are unclear in the ordinary presentation of the higher order effects, and this defect dies down if we use the $M_W - M_Z$ relation.

6. *Discussions and summary*

Studies of the electroweak higher order effects are very important for making precise tests of the theory. As a matter of fact, many authors have made efforts to calculating those effects in various processes. As a result, it is known not so easy to see the higher order effects clearly since corrections for various tree cross-sections have been found very small. Of course, it is not a negative result for the theory since those tree cross-sections are in excellent agreement with the experimental data. However, a more clean, active test is desirable.

As one of the most effective possibilities, I have examined the $M_W - M_Z$ interrelation. I have shown that the loop effects are significant while various ambiguities are small, and consequently a clean test will be possible once $M_{W,Z}$ are experimentally determined within an accuracy of 0.1–0.2 GeV. It has been also shown that the $M_W - M_Z$ relation is sensitive to the existence of heavy fermions (precisely speaking, to large mass splitting in an SU(2) doublet), and another interesting analysis will become possible: If the difference $M_Z - M_W$ is found very small, it will be interpreted as an indication of new heavy fermions. Conversely, however, if $M_Z - M_W$ is too large, it is quite difficult to explain it consistently in the framework of the standard $SU(2) \times U(1)$ electroweak theory. It may, for instance, be an indication of SU(2) triplet Higgs scalar. A great advantage of this method is that the $M_W - M_Z$ relation is derived only from the muon decay width. That is, it suffers least from complicated strong interaction effects.

Recently, the e^+e^- processes near the Z pole are also studied extensively in relation to high energy accelerators under construction: TRISTAN, SLC and LEP ([4, 47] and references therein). Further precise tests of the electroweak theory are expected to be possible since a sizable deviation from the purely electromagnetic (QED) loop effects

is predicted on the Z resonance in addition to the possibility that accurate determination of parameters, e.g., $\sin^2\theta_W$ will be made.

In comparison with the preceding analysis with the $M_W - M_Z$ relation, however, these e^+e^- processes have some theoretically unclear points although, I think, there will not be any severe difficulties in phenomenological arguments. That is, we do not know how to make systematic (well-defined) computations on the Z pole. Usually, the width Γ_Z is introduced to the Z propagator by hand otherwise we cannot make calculations, and its value is set to be $\Gamma_Z \sim 2.5$ GeV. However, this input is redundant since all independent parameters have already been fixed, and Γ_Z is a quantity which should be calculated in terms of them. Then, should the calculated Γ_Z be used? However, it is an $O(\alpha)$ quantity, so the perturbation expansion is broken if Γ_Z is used in one-loop amplitudes.

Furthermore, according to a recent work by Hollik and Timme [17], there are striking renormalization scheme differences in forward-backward asymmetry calculations in high energy $e^+e^- \to \mu^+\mu^-$ while the $M_W - M_Z$ relation receives only negligible influence. If their statement is correct, we have another support for the validity of the $M_W - M_Z$ relation, while further detailed investigations become inevitable for e^+e^- analyses.

Finally, the electroweak theory so far explained is in fact a successful theory, but we also have to recognize that it includes some theoretically unsatisfactory points, and is not the final theory. As a matter of fact, a great deal of efforts have been made seeking to go beyond the electroweak theory: Grand unification, Supersymmetrization, Composite models, ... We do not know the correct answer, but any model should reproduce the electroweak theory effectively in the region $\lesssim 10^2$ GeV. So it is almost impossible to distinguish various models by tree level analysis unless new particles characteristic of each model are directly discovered. Therefore, it is after all indispensable to make higher order analysis, and the techniques explained in this lecture are just important.

It is my great pleasure to thank the Organizing Committee of this School, especially Marek Zrałek for kind invitation and warm hospitality, and all the participants for valuable discussions. I would like to thank also B. Grządkowski for making my stay in Poland memorable and pleasant. I am grateful very much to D. Bailin for careful reading of this manuscript.

APPENDIX

A.1. Numerical check of the results

As was explicitly shown in the main text, we have to perform various complicated calculations in the studies of higher order effects. Needless to say, what is most important is to derive correct results. Unfortunately, however, it is fairly difficult to compare various results (analytical formulas) with each other directly since those formulas are usually lengthy and complicated, and several different renormalization schemes have been used. It is effective and relatively easy to do a numerical check of the results although such a check is, of course, less satisfactory than an analytical one.

In the following, I will compare our results on the weak boson masses which take very important role in the studies of the electroweak higher order effects as was explained in this lecture.

A.1.1. Calculations by Veltman [48]

In his paper, the following values for quark and Higgs masses, and the condition have been adopted:

$$m_u = m_d = 0.25, \quad m_s = 0.3, \quad m_c = 1.5, \quad m_b = 5, \quad m_t = 20$$

$$\text{and} \quad m_\phi = 200 \text{ (in GeV unit)},$$

$$R_\nu(\equiv \sigma(\bar{\nu}_\mu e \to \bar{\nu}_\mu e)/\sigma(\nu_\mu e \to \nu_\mu e))|_{E_{\nu,\bar{\nu}}=5\text{GeV}} = R_\nu^{\text{exp}}(\sin^2\theta_W = 0.238)$$

$$\Gamma(\mu \to e\nu\bar{\nu}) = \Gamma^{\text{exp}}. \tag{A.1}$$

So, I also calculated the weak boson masses under the same conditions:

	$M_W^{(0)}$	$M_W^{(1)}$	$M_Z^{(0)}$	$M_Z^{(1)}$
Veltman	76.50	78.52	87.64	90.12
Hioki	76.50	78.61	87.64	90.22

A.1.2. Calculations by Antonelli et al. [31, 49]

Their conditions are

$$m_u = m_d = 0.137, \quad m_s = 0.25, \quad m_c = 1.75, \quad m_b = 5, \quad m_t = 20$$

$$\text{and} \quad m_\phi = 10\,(\text{GeV}),$$

$$\lim_{E_{\nu,\bar{\nu}}\to 0} R_\nu = R_\nu^{\text{exp}}(\sin^2\theta_W = 0.230), \quad \Gamma(\mu \to e\nu\bar{\nu}) = \Gamma^{\text{exp}}. \tag{A.2}$$

	$M_W^{(0)}$	$M_W^{(1)}$	$M_Z^{(0)}$	$M_Z^{(1)}$
Antonelli	77.74	80.27	88.59	91.60
Hioki	77.74	80.15	88.59	91.34

A.1.3. Calculations by Böhm et al. [50][10]

They made the calculations with the same conditions as ours to do numerical check:

$$m_u = m_d = m_s = 0.1, \quad m_c = 1.5, \quad m_b = 4.7, \quad m_t = 30$$

$$\text{and} \quad m_\phi = 10\,(\text{GeV}),$$

$$R_\nu|_{E_{\nu,\bar{\nu}}=5\text{ GeV}} = R_\nu^{\text{exp}}(\sin^2\theta_W = 0.2336), \ \Gamma(\mu \to e\nu\bar{\nu}) = \Gamma^{\text{exp}}. \tag{A.3}$$

[10] I would like to thank W. Hollik for discussions.

	$M_W^{(0)}$	$M_W^{(1)}$	$M_Z^{(0)}$	$M_Z^{(1)}$
Böhm	77.14	79.4	88.11	90.7
Hioki	77.14	79.40	88.11	90.76

There is a non-negligible discrepancy on $M_Z^{(1)}$ between the present one and the one by Antonelli et al., but the agreement in the other comparisons is fairly good.

A.2. Renormalization constants

I here present the explicit expressions for the renormalization constants used in the main text. All of the constants shown below are the $O(\alpha)$ quantities in the perturbation expansion like $Z = \sum Z^{(n)}$.

A.2.1. Gauge boson field renormalization constants

$$Z_{ZZ}^{1/2} = -\frac{\alpha}{6\pi M_W^2(M_Z^2-M_W^2)}\left[\frac{N_f}{3}(8M_W^4-10M_W^2M_Z^2+5M_Z^4)-\right.$$
$$\left.-\tfrac{1}{8}(18M_W^2+2M_W^2M_Z^2-M_Z^4)\right]C_{UV}, \tag{A.4a}$$

$$Z_{AZ}^{1/2} = -\frac{\alpha}{3\pi M_W\sqrt{M_Z^2-M_W^2}}\left[\frac{N_f}{3}(8M_W^2-5M_Z^2)-\tfrac{1}{8}(30M_W^2+M_Z^2)\right]C_{UV}, \tag{A.4b}$$

$$Z_{ZA}^{1/2} = -\frac{\alpha M_W}{2\pi\sqrt{M_Z^2-M_W^2}}(C_{UV}-2\ln M_W), \tag{A.4c}$$

$$Z_{AA}^{1/2} = -\frac{\alpha}{2\pi}\left[\tfrac{1}{3}\sum_f Q_f^2(C_{UV}-2\ln m_f)-\tfrac{3}{4}(C_{UV}-2\ln M_W)-\tfrac{1}{6}\right], \tag{A.4d}$$

$$Z_W = -\frac{\alpha M_Z^2}{3\pi(M_Z^2-M_W^2)}(N_f-\tfrac{19}{8})C_{UV}, \tag{A.4e}$$

where the summation on f runs over all fermions and color degrees of freedom, and N_f is the number of generations. I have discarded all finite pieces in $Z_{ZZ}^{1/2}$, $Z_{AZ}^{1/2}$ and Z_W, because they are cancelled out when all the Feynman amplitudes are summed up and only divergent pieces are necessary to get finite amplitudes in intermediate stages.

A.2.2. Gauge boson mass renormalization constants

$$\delta M_Z^2 = \frac{\alpha M_Z^2}{4\pi M_W^2(M_Z^2-M_W^2)}\left[\tfrac{4}{9}N_f(5M_Z^4-10M_Z^2M_W^2+8M_W^4)\right.$$

$$-\tfrac{1}{2}M_Z^2\sum_f m_f^2+\tfrac{1}{6}(7M_Z^4+10M_Z^2M_W^2-42M_W^4)\Big]C_{UV}$$

$$-\frac{\alpha}{8\pi M_W^2(M_Z^2-M_W^2)}\Big[\sum_f M_Z^4\{M_Z^2(\eta_f^2+1)F(m_f,m_f,M_Z)-m_f^2F_0(m_f,m_f,M_Z)\}$$

$$-\frac{M_Z^2}{3}(M_Z^4-2M_Z^2M_W^2+4M_W^4)+M_Z^6\ln M_Z+2M_W^2(M_Z^4-4M_Z^2M_W^2+16M_W^4)\ln M_W$$

$$+M_Z^2(M_Z^4-4M_Z^2M_W^2+24M_W^4)F(M_W,M_W,M_Z)$$

$$+M_W^2(3M_Z^4-14M_Z^2M_W^2-16M_W^4)F_0(M_W,M_W,M_Z)$$

$$+M_Z^6\{2F_0(m_\phi,M_Z,M_Z)-F_2(m_\phi,M_Z,M_Z)\}$$

$$-m_\phi^2M_Z^4\{F_1(M_Z,m_\phi,M_Z)-\ln m_\phi\}\Big], \tag{A.5a}$$

$$\delta M_W^2=-\frac{\alpha M_Z^2}{24\pi(M_Z^2-M_W^2)}\Big[\sum_{(I,i)}|U_{Ii}|^2(3m_I^2+3m_i^2-2M_W^2)+31M_W^2-6M_Z^2\Big]C_{UV}$$

$$-\frac{\alpha}{8\pi(M_Z^2-M_W^2)}\Big[2M_Z^2\sum_{(I,i)}|U_{Ii}|^2\{2M_W^2F(m_I,m_i,M_W)$$

$$-m_i^2F_1(m_I,m_i,M_W)-m_I^2F_1(m_i,m_I,M_W)\}$$

$$-M_Z^2M_W^2(1-14\ln M_W)+M_Z^2(12M_W^2+M_Z^2)\ln M_Z$$

$$+\{(M_Z^4-20M_Z^2M_W^2-8M_W^4)F_0(M_Z,M_W,M_W)$$

$$+(M_Z^4+16M_Z^2M_W^2+4M_W^4)F_1(M_Z,M_W,M_W)-M_W^2(M_Z^2+20M_W^2)F_2(M_Z,M_W,M_W)\}$$

$$-4M_W^2(M_Z^2-M_W^2)\{2F_0(0,M_W,M_W)-F_1(0,M_W,M_W)+5F_2(0,M_W,M_W)\}$$

$$+m_\phi^2M_Z^2\{\ln m_\phi-F_1(M_W,m_\phi,M_W)\}$$

$$+M_Z^2M_W^2\{2F_0(m_\phi,M_W,M_W)-F_2(m_\phi,M_W,M_W)\}\Big], \tag{A.5b}$$

where η_f, F_n $(n=0,1,2)$ and F are defined in Sect. 3.1.

A.2.3. Lepton field renormalization constants

$$Z_L^\nu=-\frac{\alpha M_Z^2}{16\pi M_W^2(M_Z^2-M_W^2)}\{(2M_W^2+M_Z^2)(C_{UV}-\tfrac{1}{2})-4M_W^2\ln M_W-2M_Z^2\ln M_Z\}, \tag{A.6a}$$

$$Z_L^1 = -\frac{\alpha}{4\pi}\left\{C_{UV}+4\ln\lambda+4-6\ln m_l+\frac{M_Z^2}{2(M_Z^2-M_W^2)}(C_{UV}-\tfrac{1}{2}-2\ln M_W)\right.$$
$$\left.+\frac{(M_Z^2-2M_W^2)^2}{4M_W^2(M_Z^2-M_W^2)}(C_{UV}-\tfrac{1}{2}-2\ln M_Z)\right\}, \tag{A.6b}$$

$$Z_R^1 = -\frac{\alpha}{4\pi}\left\{C_{UV}+4\ln\lambda+4-6\ln m_l+\frac{M_Z^2-M_W^2}{M_W^2}(C_{UV}-\tfrac{1}{2}-2\ln M_Z)\right\}. \tag{A.6c}$$

A.2.4. Charge renormalization constant

We have to evaluate first the one-loop-corrected eeA vertex. Then, by combining this vertex at $q^2 = 0$ and the corresponding counterterm (which consists of $Z_{AA}^{1/2}$, $Z_{ZA}^{1/2}$, $Z_{L,R}^e$ and Y), Y is determined through the on-mass-shell condition.

$$Y = -\frac{\alpha}{4\pi}\left[\tfrac{7}{2}(C_{UV}-2\ln M_W)+\tfrac{1}{3}-\tfrac{2}{3}\sum_f Q_f^2(C_{UV}-2\ln m_f)\right]. \tag{A.7}$$

REFERENCES

[1] S. L. Glashow, *Nucl. Phys.* **22**, 579 (1961); S. Weinberg, *Phys. Rev. Lett.* **19**, 1264 (1967); A. Salam, in: *Elementary Particle Theory*, ed. N. Svartholm, Almqvist and Wiksell, Stockholm 1968, p. 367; S. L. Glashow, J. Iliopoulos, L. Maiani, *Phys. Rev.* **D2**, 1285 (1970); M. Kobayashi, T. Maskawa, *Prog. Theor. Phys.* **49**, 652 (1973); Review articles: E. S. Abers, B. W. Lee, *Phys. Rep.* **9C**, 1 (1973); M. A. B. Bég, A. Sirlin, *Phys. Rep.* **88**, 1 (1982); C. Quigg, in.: *Gauge Theories of the Strong, Weak, and Electromagnetic Interactions*, Benjamin, Reading, MA 1983.

[2] UA1 Collaboration: G. Arnison et al., *Phys. Lett.* **122B**, 103 (1983); **126B**, 398 (1983); **129B**, 273 (1983); **134B**, 469 (1984); **166B**, 484 (1986); UA2 Collaboration: M. Banner et al., *Phys. Lett.* **122B**, 476 (1983); P. Bagnaia et al., *Phys. Lett.* **129B**, 130 (1983); *Z. Phys.* **C24**, 1 (1984); J. A. Appel et al., *Z. Phys.* **C30**, 1 (1986).

[3] T. W. Appelquist, J. R. Primack, H. R. Quinn, *Phys. Rev.* **D6**, 2998 (1972); and **D7**, 2998 (1973); D. A. Ross, *Nucl. Phys.* **B51**, 116 (1973); A. Sirlin, *Nucl. Phys.* **B71**, 29 (1974); P. Salomonson, Y. Ueda, *Phys. Rev.* **D11**, 2606 (1975).

[4] B. W. Lynn, J. F. Wheater, ed.: *Workshop on Radiative Corrections in $SU(2)_L \times U(1)$*, Trieste 1983, World Scientific, Singapore 1984.

[5] K-I. Aoki, Z. Hioki, R. Kawabe, M. Konuma, T. Muta, *Prog. Theor. Phys. Suppl.* No. 73 (1982).

[6] K-I. Aoki, Z. Hioki, R. Kawabe, M. Konuma, T. Muta, *Prog. Theor. Phys.* **64**, 707 (1980).

[7] K-I. Aoki, Z. Hioki, R. Kawabe, M. Konuma, T. Muta, *Prog. Theor. Phys.* **65**, 1001 (1981).

[8] K-I. Aoki, Z. Hioki, *Prog. Theor. Phys.* **66**, 2234 (1981).

[9] Z. Hioki, *Prog. Theor. Phys.* **67**, 1165 (1982).

[10] Z. Hioki, *Prog. Theor. Phys.* **68**, 2134 (1982).

[11] Z. Hioki, *Prog. Theor. Phys.* **71**, 663 (1984).

[12] F. Halzen, Z. Hioki, M. Konuma, *Phys. Lett.* **126B**, 129 (1983).

[13] Z. Hioki, *Nucl. Phys.* **B229**, 284 (1983).

[14] Z. Hioki, in: Proceedings of the International Symposium on Physics of Proton-Antiproton Collision, Univ. of Tsukuba and National Lab. for High Energy Physics (KEK), Tsukuba, Japan, March 13–15, 1985, eds. Y. Shimizu and K. Takikawa (KEK, 1985), p. 223.

[15] K. Inoue, A. Kakuto, H. Komatsu, S. Takeshita, *Prog. Theor. Phys.* **64**, 1008 (1980); D. Yu. Bardin, P. Ch. Christova, O. M. Fedorenko, *Nucl. Phys.* **B197**, 1 (1982).
[16] S. Sakakibara in Ref. [4].
[17] W. Hollik, H.-J. Timme, Preprint DESY 85-099.
[18] G. 't Hooft, M. Veltman, *Nucl. Phys.* **B44**, 189 (1972).
[19] H. Czyż, J. Sładkowski, M. Zrałek, Jagellonian Univ. (Cracow) preprint TPJU-3/85.
[20] A. Sirlin, *Phys. Rev.* **D22**, 971 (1980).
[21] N. Nakanishi, *Prog. Theor. Phys.* **19**, 159 (1958); T. Kinoshita, *J. Math. Phys.* **3**, 650 (1962); T. D. Lee, M. Nauenberg, *Phys. Rev.* **133**, B1549 (1964).
[22] S. M. Berman, *Phys. Rev.* **112**, 267 (1958); T. Kinoshita, A. Sirlin, *Phys. Rev.* **113**, 1652 (1959).
[23] N. Byers, R. Rückl, A. Yano, *Physica* **96A**, 163 (1979); M. Green, M. Veltman, *Nucl. Phys.* **B169**, 137 (1980); and **B175**, 547E (1980); M. Green, *J. Phys. G: Nucl. Phys.* **7**, 1169 (1981); S. Sarantakos, A. Sirlin, W. J. Marciano, *Nucl. Phys.* **B217**, 84 (1983).
[24] J. E. Kim, P. Langacker, M. Levine, H. H. Williams, *Rev. Mod. Phys.* **53**, 211 (1981); F. Dydak, *Philos. Trans. R. Soc. London* **A304**, 43 (1982).
[25] L. Maiani, in: Proceedings of the International Conference on Unified Theories and Experimental Tests, Venice, Italy, March 16–18, 1982, Inst. Naz. Fis. Nucl. Italy 1983, p. 55.
[26] a) W. Wetzel, *Z. Phys.* **C11**, 117 (1981). b) W. J. Marciano, A. Sirlin, *Phys. Rev.* **D29**, 945 (1984); and **D31**, 213E (1985).
[27] N. Cabibbo, R. Gatto, *Phys. Rev.* **124**, 1577 (1961); F. A. Berends, G. J. Komen, *Phys. Lett.* **63B**, 432 (1976); M. Igarashi, N. Nakazawa, T. Shimada, Y. Shimizu, *J. Phys. Soc. Jpn.* **51**, 2393 (1982); B. W. Lynn, G. Penso, C. Verzegnassi, Preprint SLAC-PUB-3742; F. Jegerlehner, *Z. Phys.* **32C**, 195 (1986).
[28] F. Antonelli, G. Corbò, M. Consoli, O. Pellegrino, *Nucl. Phys.* **B183**, 195 (1981).
[29] M. Consoli, S. Lo Presti, L. Maiani, *Nucl. Phys.* **B223**, 474 (1983).
[30] Mark J Collaboration: B. Adeva et al., *Phys. Rev. Lett.* **54**, 1750 (1985); A. J. Buras, in: Proceedings of the 1981 International Symposium on Lepton and Photon Interactions at High Energies, Univ. of Bonn, 24–29 August, 1981, ed. W. Pfeil, p. 636.
[31] W. J. Marciano, A. Sirlin, *Phys. Rev. Lett.* **46**, 163 (1981).
[32] C. Verzegnassi, *Phys. Lett.* **147B**, 455 (1984); N. A. Papadopoulos, J. A. Peñarrocha, F. Scheck, K. Schilcher, *Phys. Lett.* **149B**, 213 (1984); and *Nucl. Phys.* **B258**, 1 (1985).
[33] W. J. Marciano, *Phys. Rev.* **D20**, 274 (1979); S. Dawson, J. S. Hagelin, L. Hall, *Phys. Rev.* **D23**, 2666 (1981); F. Antonelli, L. Maiani, *Nucl. Phys.* **B186**, 269 (1981); S. Bellucci, M. Lusignoli, L. Maiani, *Nucl. Phys.* **B189**, 329 (1981).
[34] Y. Kazama, Y-P- Yao, *Phys. Rev.* **D21**, 1116 (1980); **D21**, 1138 (1980); and **D25**, 1605 (1982).
[35] A. Sirlin, *Phys. Rev.* **D29**, 89 (1984).
[36] UA1 Collaboration: G. Arnison et al., *Phys. Lett.* **147B**, 493 (1984).
[37] B. Grządkowski, P. Krawczyk, J. Pawełczyk, S. Pokorski, Preprint CERN-TH. 4041/84.
[38] K-I. Aoki, H. Aoyama, *Nucl. Instrum. Methods* **A248**, 483 (1986).; *Z. Phys.* **C31**, 557 (1986).
[39] T. Appelquist, J. Carazzone, *Phys. Rev.* **D11**, 2856 (1975).
[40] S. Bertolini, A. Sirlin, *Nucl. Phys.* **B248**, 589 (1984).
[41] A. C. Longhitano, *Phys. Rev.* **D22**, 1166 (1980).
[42] J. Van der Bij, M. Veltman, *Nucl. Phys.* **B231**, 205 (1984); J. J. Van der Bij, *Nucl. Phys.* **B248**, 141 (1984).
[43] M. Veltman, *Nucl. Phys.* **B123**, 89 (1977); See also: M. B. Einhorn, D. R. T. Jones, M. Veltman, *Nucl. Phys.* **B191**, 146 (1981).
[44] M. Davier, in: Proceedings of the 21st International Conference on High Energy Physics, Paris 1982, eds. P. Petiau and M. Porneuf; *J. Phys.* (France) **43** (1982); Colloque C3-471; L. Maiani, in: Colloque C3-631.
[45] J. Fleischer, F. Jegerlehner, *Nucl. Phys.* **B228**, 1 (1983).
[46] A. Sirlin, W. J. Marciano, *Nucl. Phys.* **B189**, 442 (1981).

[47] G. Passarino, M. Veltman, *Nucl. Phys.* **B160**, 151 (1979); M. Consoli, *Nucl. Phys.* **B160**, 208 (1979); F. A. Berends, R. Kleiss, S. Jadach, *Nucl. Phys.* **B202**, 63 (1982); M. Böhm, W. Hollik, *Nucl. Phys.* **B204**, 45 (1982); W. Wetzel, *Nucl. Phys.* **B227**, 1 (1983); M. Igarashi, N. Nakazawa, T. Shimada, Y. Shimizu, *Nucl. Phys.* **B263**, 347 (1986); B. Grządkowski, P. Krawczyk, J. H. Kühn, R. G. Stuart, *Phys. Lett.* **163B**, 247 (1985); K. Tobimatsu, Y. Shimizu, *Prog. Theor. Phys.* **74**, 567 (1985); Preprint KEK 85–59; B. W. Lynn, M. E. Peskin, R. G. Stuart, Preprint SLAC-PUB-3725.

[48] M. Veltman, *Phys. Lett.* **91B**, 95 (1980).

[49] F. Antonelli, M. Consoli, G. Corbò, *Phys. Lett.* **91B**, 90 (1980).

[50] M. Böhm, W. Hollik, H. Spiesberger, *Z. Phys.* **C27**, 523 (1985).